NUMERICAL MODELING OF WELLBORE INSTABILITY (SHEAR FAILURE) USING FRACTURE MECHANICS APPROACH

BY

KALU, Ifeanyi Emmanuel

A THESIS

SUBMITTED TO THE AFRICAN UNIVERSITY OF SCIENCE AND TECHNOLOGY

ABUJA – NIGERIA

IN PARTIAL FULFILLMENT OF THE REQUIREMENTS FOR THE

AWARD OF MASTER OF SCIENCE IN MATERIALS SCIENCE AND ENGINEERING

SUPERVISOR: PROF. WINSTON O. SOBOYEJO

MAY 2013

NUMERICAL MODELING OF WELLBORE INSTABILITY (SHEAR FAILURE) USING FRACTURE MECHANICS APPROACH

A THESIS APPROVED

BY

SUPERVISOR: _____

PROF. WINSTON O. SOBOYEJO

DEDICATION

This thesis is dedicated to my family,

my mum, Mrs. Ada Uduma Kalu,

and to my one and only sister, Miss Ugo Grace Kalu.

ACKNOWLEDGEMENTS

All praises and glory be to Almighty God for giving me the inspiration and enablement to do this study. I remain grateful to Him.

My sincere appreciation goes to my supervisor, Prof. Wole Soboyejo for being there for me all through the period of my masters program. Thank you for exposing me to the fundamentals of materials science and engineering, and mechanical behaviour of materials, which arouse the drive to embark on this study. I remain grateful for the guidance and encouragement you gave me in the course of this work. In a null shell, I will say you really made a remarkable impact in my life beyond the spheres of academics. Thank you.

I will like to extend me appreciation to Dr. Alpheus Igbokoyi for the insights and technical contributions he made to this work. Thank you for all your comments, advice and suggestions.

My gratitude further goes to my research partner, Elijah Jossou. Your great contributions to the success of this work will never be forgotten. Thank you for all the time you gave in praying and brainstorming together with me on this work. Please accept my heartfelt appreciation.

I am also grateful to Mr Omotayo Omosebi for exposing me to the fundamentals of wellbore stability and other petroleum related issues of this work. I will also like to say a big thank you to Mr Haruna Onuh for his passion towards ensuring that this work is successful. He was always there each time I call on him. When all hope was lost in getting a data to work with, he amazingly went out of his way to provide the oil field data used for this work. I cannot but say am grateful.

This acknowledgement will be incomplete without expressing my profound gratitude to Mr Kehinde Oyewole and Mr Idris Malik (my roommate), for the support, suggestions, and technical assistance they gave me on the use of ABAQUS while doing this work. Thank you for brainstorming with me on different aspects of this work. You guys were indeed wonderful. Please do accept my appreciation.

I will like to appreciate Mr Arthur Emmanuel for his tips of suggestions in this work. My thanks also go to the all multifunctional group members, led by Mr Ebenezar Annan, for their valuable contributions to this work.

Finally, I will express my appreciation to my family for their continuous encouragement all through my masters program. They have always been there for me in all aspects of life.

ABSTRACT

Wellbore instabilities are responsible for 10-20% of the total drilling cost. It has been estimated that wellbore instability causes an annual economic loss of US$ 500 - 1000 million in the oil industry across the world. Hence, the maintenance of wellbore stability is of major concern to drilling engineers in the oil and gas industry. Hence, several models have been developed for the assessment or prediction of wellbore instabilities. However, these models do have some limitations. They often require the use of mechanical property data that is relatively difficult to generate in the field, as most rely on mechanical property measurements typically obtained from core samples that are costly to extract. Most of the existing models require parameters that can only be obtained through complicated and difficult laboratory testing. Even when the data is available, the often exhaustive list of input data required by the models may be difficult to relate to wellbore stability. Furthermore, the conventional strength based models neglects the existence of pre-existing cracks in the rock formations which can remarkably affect the stability of well bores when subjected to various stresses. There is, therefore, a need to develop new approaches that are easier to implement. The models must also address limitations of the existing models and serve as a guide for the assessment or prediction of well bore instability.

This study presents a numerical modeling of wellbore instability (shear failure) using fracture mechanics approach. A typical well bore consists of various layers of rock formations having inherent cracks and distinct mechanical properties. Using the concept of linear elastic fracture mechanics (LEFM), the wall of a distinct layer of the wellbore containing cracks of various sizes (ranging from 0.5” to 2.5”) inclined at a particular angle and subjected to a range of bottom hole pressure (3000 – 7000 psi) was numerically modeled using the ABAQUS software package. The insights from these models were used to guide the prediction of the onset of shear failure wellbore instability and consequently the determination of the lower bound mud weight window for safe drilling operations in conventional wells.

TABLE OF CONTENTS

LIST OF FIGURES

LIST OF TABLES

CHAPTER ONE

1.0 Introduction

1.1 Background and Motivation

Maintenance of wellbore stability is of major concern to drilling engineers in the oil and gas industry [1] since wellbore instability has been the primary cause of financial losses in boreholes in the drilling industry [2]. Wellbore instabilities are responsible for 10-20% of the total drilling cost [3]. It has been estimated that wellbore instability causes an annual economic loss of US$ 500 - 1000 million in the oil industry across the world [4].

Wellbore stability is of critical importance for both the drilling process and production stage because it is highly desirable to have an intact wellbore that is functional and fit for the purpose for which it was drilled. A damaged wellbore can impair use, resulting in loss circulation in regions with high tensile stresses [2, 5]. It may also lead to breakouts and hole closures in cases of compressive and shear failures [2, 5]. In severe cases, wellbore instability can lead to stucked or damaged drill pipes, and eventually, loss of the open-hole sections. Hence, borehole instability problems result in large economic losses to the operating company and its investors [2].

The safe drilling of horizontal and conventional wells (through rock formations) requires a framework for the modeling of stability in layered rock structures with properties that vary significantly over the depths of the wells [5]. The modeling approaches that are available for the prediction or assessment of wellbore instability risks include: analytical and semi-analytical constitutive models (such as linear elastic, elastoplastic, and poroelastic models) [6, 7], and failure criteria models (such as Mohr-Coulomb, Drucker-Prager, and modified Lade criteria) [6], geomechanical models [6], numerical models (such as finite element method, FEM, finite difference method, FDM, boundary element method, BEM) [6] and laboratory model analogues, which include thick-walled cylinders and borehole collapse tests [6].

However, the prediction of borehole stability is limited by the significant variations in rock mechanical properties over the large distances that are typically involved in the drilling of oil and gas wells. These mechanical property measurements are typically obtained from core samples that are expensive to extract. They also use complicated and difficult conventional mechanical

testing methods and costly wireline /electric logging [5, 7]. Hence, the modeling of wellbore instability often requires the use of mechanical property data that is relatively difficult to generate in the field. Even when the data is available, the often exhaustive list of input data required by the models may be difficult to relate to wellbore stability [4, 7]. Furthermore, the conventional strength based models neglects the existence of pre-existing cracks in the rock formations which can remarkably affect the stability of well bores when subjected to various stresses. There is, therefore, a need to develop new approaches that are easier to implement. These models must also address limitations of the existing models and serve as a guide for the assessment or prediction of well bore instability.

1.2 Research Objectives

The primary objective of this work is to develop a numerical model for the prediction of shear failure in wellbore using ABAQUS and linear elastic fracture mechanics concept. Furthermore, to obtain the lower bound mud weight window that can be used for safe drilling operations.

1.3 Scope of Research

In this work, a typical wellbore will be considered to consist of various layers of rock formations having inherent cracks and distinct mechanical properties. A distinct layer of the wellbore containing cracks of various sizes (assumed to be inclined at a particular angle) and subjected to a range of bottom hole pressure will be numerically modeled using the ABAQUS software package. The concept of linear elastic fracture mechanics (LEFM) will be assumed in this study. This simplicity provides a conservative approach to predict the drilling pressure for the onset of shear failure of wellbores. The insights from this model will then be used to guide the development of concepts for the determination of lower bound mud weight window for safe drilling operations in conventional wells.

1.4 Outline of Thesis

This chapter presents the background and motivation, as well as the objectives and scope of the research. Chapter 2 then presents a review of relevant literature. Subsequently, the numerical modeling of shear failure in a typical wellbore using fracture mechanics approach will be described in chapter 3 before presenting the results in chapter 4. Salient conclusions arising from the work are summarized in chapter 5 along with suggestions for future work.

1.5 References

[1] Chen, S., "Analytical and Numerical Analyses of Wellbore Drilled in Elastoplastic Porous Formations", *Dissertation submitted to the graduate faculty, University of Oklahoma, USA*, pp. 1-2, 2012.

[2] Lang J., Li S., Halliburton USA, Zhang J., Shell Exploration & Production Company, USA, "Wellbore Stability Modeling and Real-Time Surveillance for Deepwater Drilling to Weak Bedding Planes and Depleted Reservoirs", *SPE/IADC 139708*, 1-18, 2011.

[3] Santarelli F. J., Chenevert M. E., Osisanya S. O., "On the Stability of Shales and Its Consequences in Terms of Swelling and Wellbore Stability", *Presented as SPE/IADC 23886 at SPE/IADC Drilling Conference*, New Orleans, LA, Feb. 18-21, 1992.

[4] Chen G., Chenevert M. E., Sharma M. M., Yu, M., "A Study of Wellbore Stability in Shales Including Poroelastic, Chemical, and Thermal Effects", *Journal of Petroleum Science and Engineering 38*:167-176, 2003.

[5] Igbokoyi A., Rahbar N., Soboyejo W., "Rock Mechanical Properties for Borehole Stability Modeling in Niger Delta Region", *Research Proposal Submitted to Petroleum Technology Development Fund (PTDF), Nigeria*, pp. 1-18, 2012.

[6] McLellan, P.J., "Assessing the Risk of Wellbore Instability in Horizontal and Inclined Wells", *The Journal of Canadian Petroleum Technology, Vol. 35, No. 5*, 21-32, 1996.

[7] Volk L., Carroll H., "Status Report on Modeling of Wellbore Stability", *U.S. Department of Energy, Bartlesville Project Office, Oklahoma, USA, NIPER/BDM-0199*, pp. 1-6, 1995.

CHAPTER TWO

2.0 Literature Review

2.1 Wellbore Stability

The integrity of the borehole plays an important role in many well operations [1]. Wellbore stability is a major concern during drilling for oil and gas. Shales make up over 75% of drilled formations and are responsible for more than 90% of wellbore instability problems [2]. These instabilities are responsible for 10-20% of the total drilling cost, with a conservative estimated cost to the industry of US$500 million per year [3].

The oil and gas industry continues to fight borehole problems. The problems include: hole collapse, tight holes, stuck pipes, poor hole cleaning, hole enlargement, plastic flow, fracture, and lost circulation [4]. Most of these borehole problems that drive up drilling costs are related to wellbore stability. These problems are mainly caused by the imbalance created between the rock (shale) stresses and strengths after wellbore drilling [4].

Wellbore stability is a term used in the oil and gas industry to describe usable condition of the borehole during drilling operations. A usable hole must successfully accommodate logging or any open-hole evaluation, casing run and any other drilling activities [5]. Wellbore instability is recognized when the hole diameter is markedly different from the bit size and the hole does not maintain its structural integrity, as shown below in Figure 2.1 [6].

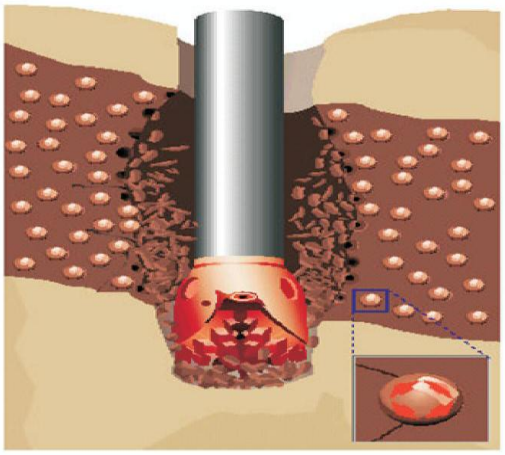

Figure 2.1: Schematic Illustration of Wellbore Instability (Adapted from [6])

Before a well is drilled, pore pressure and compressive stresses exist within the rock (shale) formations. With the exception of structurally complex areas (e.g. near salt diapirs), the *in-situ* stresses can be resolved into a vertical stresses, (σ_v) , and the horizontal stresses $(\sigma_H \; and \; \sigma_h)$, which are generally unequal but are in equilibrium with the shale strength. When the well is drilled, the balance between the stress and shale strength is disturbed. Consequently, the stresses are altered in the vicinity of the wellbore and are redistributed, as the support originally offered by the drilled out shale is partially replaced by the hydraulic pressure of the drilling mud. The redistributed stresses are normally referred to as the hoop (or tangential) stress, σ_t , which act circumferentially around the wellbore wall, the radial stress, $\sigma_{r,}$ and the axial stress, $\sigma_{a,}$ which act parallel to the wellbore axis are illustrated in Figure 2.2 and Figure 2.3 [4,7].

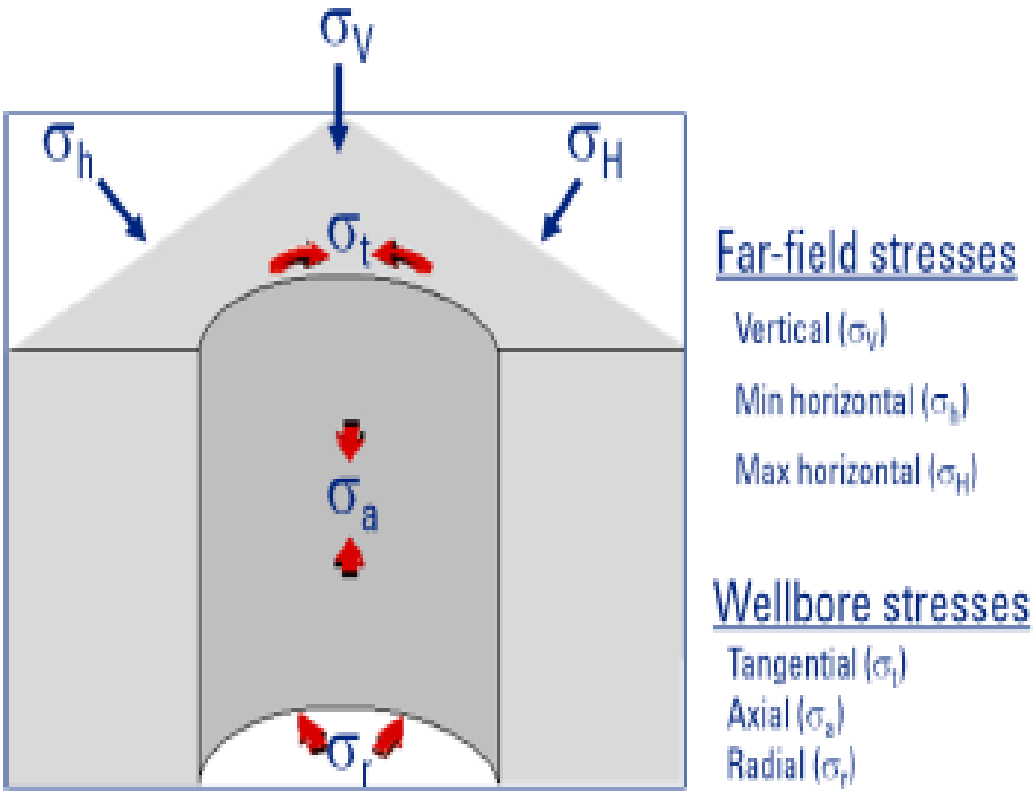

Figure 2.2: Redistribution of Stresses near Wellbore Wall (Adapted from [7])

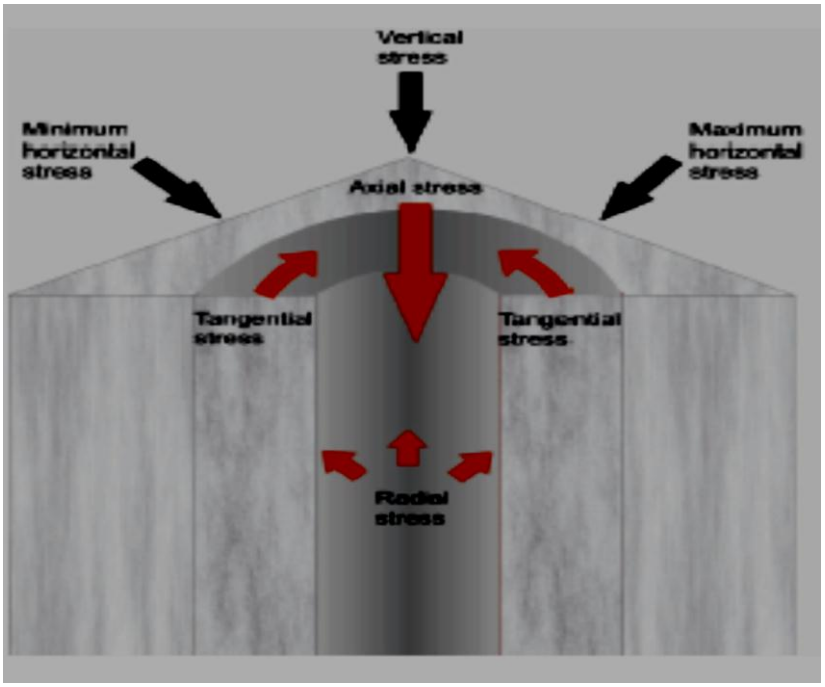

Figure 2.3: Wellbore Stresses during Drilling (Adapted from [12])

If the redistributed stress-state exceeds the shale strength, instability may result. This type of instability is referred to as **mechanical instability** [6]**.** Also, as drilling progresses, the interaction of the drilling fluid with the shales alters the shale strength, as well as the pore pressures adjacent to the borehole wall. Shale strength normally decreases and pore pressure increases as fluid enters the shale, leading to another type of instability known as **chemical instability**. This usually causes the borehole to collapse with time [4].

Mechanical instability occurs as soon as the new formation is drilled. However, chemical instability is time dependent because shales are subject to strength alteration, once exposed to different fluids. Despite the tendency of shales to experience chemical instability, they may also experience mechanical instability simultaneously. This can lead to more complex problems that include; hole collapse, stuck pipes, lost circulation, and well break out. Hence, in this work, only mechanical wellbore instability will be examined [8].

Mechanical instability takes place when the redistributed stresses exceed the shale strength. Borehole failure can be broadly classified as being either tensile or compressive [5]. Tensile failure (or fracturing) occurs when the wellbore pressure (from the drilling fluid) exceeds the tensile strength of the shale. This can lead to lost circulation (fluid losses) [5, 9]. On the other

hand, compressive or shear failure occurs when there is insufficient wellbore fluid pressure support. This can lead to "sloughing" in brittle formations (resulting in wellbore enlargement), wellbore breakout, spalling, and cave-in [5, 9].

In general, the borehole stability problems can be grouped into the following four categories according to the mud-weight magnitudes (refer to Figure 2.4):

- Wellbore washouts or kicks owing to underbalanced drilling (which can lead to a blow-out), where the mud weight is far less than pore pressure, or as a result of drilling in unconsolidated or weak formations.
- Breakouts or shear failures owing to low mud weight.
- Losses or loss circulation from high mud weight.
- Failure or sliding related to pre-existing fractures or drilling-induced formation damage.

Figure 2.4 illustrates the relationships between mud weight, wellbore stability, and various rock failures. When the mud pressure is less than the pore pressure, the wellbore failure occurs by splintering or spalling. When the mud pressure is less than the shear failure gradient, the wellbore exhibits shear failure or break out. If the mud pressure is too high, drilling-induced hydraulic fractures are generated, which may cause loss of drilling mud. Hence, to maintain wellbore stability, the mud weight must be in the appropriate range [10].

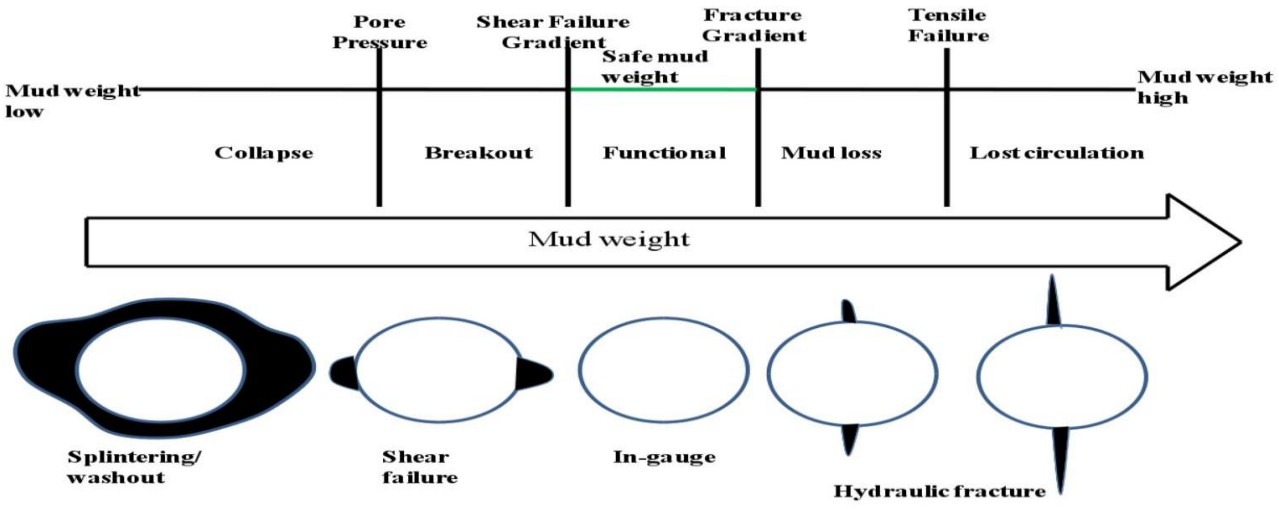

Figure 2.4: Schematic Illustration of the Relationship between Mud Pressure (Mud weight) and Wellbore Failures (Adapted from [5])

To prevent borehole instability, there is a need to restore the balance between the new stress and the strength environment. Factors that affect the effective stress include: wellbore pressure (from the mud weight of the drilling fluid); shale pore pressure; far-field *in-situ* stresses; trajectory and hole angle. The effective stress at any point on or near the borehole is described in terms of the three principal stress components. These include: a radial stress component (σ_r) that acts along the radius of the wellbore, a hoop/tangential stress (σ_t), an axial stress (σ_a) acting parallel to the well path, and additional shear stress components [4].

To prevent shear failure, the shear stress-state obtained from the difference between the stress components (hoop – usually the largest and radial stress – smallest), should not exceed the shear strength failure envelope. To prevent failure due to tensile stresses, the hoop stress should not exceed the tensile strength of the rock [4].

Mechanical stability problem can be prevented by restoring the stress-strength balance through adjustment of mud weight and effective circulation density (ECD) through drilling/tripping practices, and trajectory control. Chemical instability can be prevented through selection of proper drilling fluids, suitable mud additives to minimize/delay the fluid/shale interactions, and by reducing the shale exposure time. The selection of appropriate drilling mud with suitable additives can even generate fluid flow from shale into the wellbore, reducing near wellbore pressure and preventing shale strength reduction [4].

2.2 Symptoms of Wellbore Instability

Table 2.1 summarizes the symptoms of wellbore instability [11]. These are caused primarily by wellbore collapse or convergence during drilling, completion or production of a well. Observations of over-gauge or under-gauge holes, as readily seen from caliper logs are the most direct symptoms of instability. Cavings from the wellbore wall, circulated to the surface, and hole fill after tripping do show that spalling processes occur in the wellbore. Hole enlargement is confirmed by large volumes of cuttings and/or cavings, in excess of the volume of rock which would have been excavated in a gauge hole. So, if the fracture gradient is not exceeded and naturally fractured formations are not encountered, a requirement for cement volumes in excess

of the calculated drilled hole volume is also a direct indication that enlargement has occurred [11, 12].

Several indirect symptoms of wellbore instability, which may not necessarily be as a result of wellbore collapse or convergence alone, are presented in Table 2.1. In quite a number of cases, these symptoms are usually taken to be mechanical or drilling fluid-related causes. Hence, they are not clear symptoms of well instability and rock detachment. Well collapse or convergence, especially in inclined or horizontal holes are usually characterized by high torque and drag friction, stuck pipe or coiled tubing, the hanging up of the drill-string, casing, tubing or logging tools [11]. Excessive doglegs and keyhole seating may result from selective hole enlargement in some formations that are drilled at inclined angles. Wellbore instability may also be characterized by increased circulation pressures due to hole rugosity, partial convergence, and increased mud densities (due to the addition of caved material).

Deterioration of the drilling fluid properties, and hence hole cleaning capability due to excess solids in the mud, is another sign of instability. When a drill-spring's resonant frequency is attained in a progressively failing wellbore, drill-string vibrations and in some extreme cases, fatigue failure of the drill-pipe may result from hole enlargement. As a consequence of excessive hole enlargement, poor logging responses, poor cementing due to low displacement velocities and mud contaminations, and ultimately poor perforation penetration may occur [11,12].

Table 2.1: Symptoms of Wellbore Instability Due to Wellbore Collapse or Convergence

DIRECT SYMPTOMS	**INDIRECT SYMPTOMS**
Oversize hole (caliper logs)	High torque and drag friction
Undergauge hole	Stuck pipe and deviation control problems
Excessive volume of cuttings and cavings	Hanging up of drill-string, casing, or coiled tubing
Cavings at surface	Increased circulating pressures
Hole fill after tripling	Excessive drill-string vibrations
Excess cement volume required	Drill-string failure
	Excessive doglegs and keyhole seating
	Annular gas leakage due to poor cement job
	Poor logging response and inability to run logs

2.3 Causes of Wellbore Instability

Wellbore instability is usually caused by factors that may be classified as uncontrollable (natural) or controllable factors, as shown in Table 2.2 [11, 12, 13].

Table 2.2: Causes of Wellbore Instability

Controllable Factors	**Uncontrollable (Natural) Factors**
Bottom hole pressure (Mud density)	Naturally fractured or faulted formations
Well inclination	Tectonically stressed formations
Transient pore pressures	High in-situ stresses
Physical/chemical rock-fluid interaction	Mobile formations
Drill-string vibrations	Unconsolidated formations
Erosion	Naturally over-pressurized shale collapse
Temperature	Induced over-pressurized shale collapse

2.3.1 Uncontrollable (Natural) Factors

2.3.1.1 Naturally Fractured or Faulted Formations

Figure 2.5 shows an example of a naturally fractured or faulted formation. A natural fracture system in rocks can often be found near faults [12]. Such rocks can be broken into large or small pieces. If they are loose, they can fall into the wellbore and jam the string in the hole. Hole collapse problems may become quite severe if weak bedding planes intersect a wellbore at unfavorable angles. Such fractures in shales may provide a pathway for mud or fluid invasion that can lead to the time-dependent degradation of the rock strength and stiffness, as well as softening and ultimately to hole collapse. Highly fractured zones particularly in the vicinity of faults may also result in large volumes of rock falling into the wellbore [11, 12].

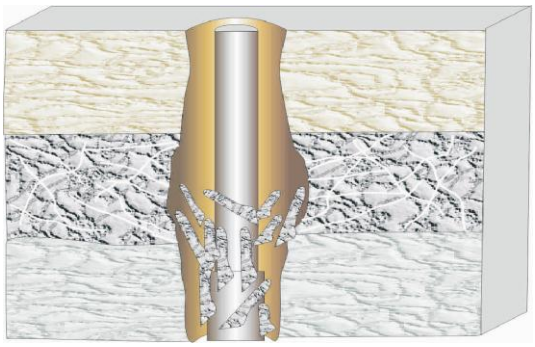

Figure 2.5: Drilling through Naturally Fractured or Faulted Formations (Adapted from [12])

2.3.1.2 Tectonically Stressed Formations

Tectonic stresses build up in areas where rocks are being compressed or stretched as a result of the earth's crust movement. The rocks in these areas buckle due to the pressure of the moving tectonic plates. Wellbore instability can occur when these highly stressed formations are drilled and if there is a significant difference between the near wellbore stress and the restraining pressure provided by the drilling fluid density. As a result of drilling a hole in these areas, the rocks around the wellbore wall collapse into the wellbore and produce splintery cavings, like those produced by over-pressured shale (see Figure 2.6). This usually occurs in or near mountainous regions, whereby the hydrostatic pressure required to stabilize the wellbore may be far higher than the fracture pressure of the other exposed formations [12].

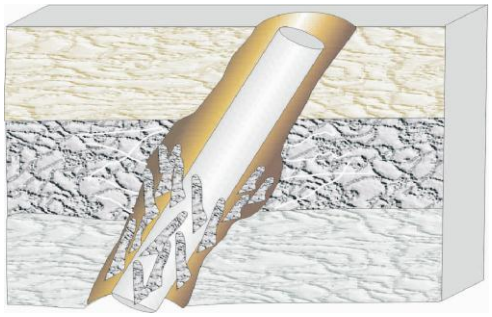

Figure 2.6: Drilling through Tectonically Stressed Formations (Adapted from [12])

2.3.1.3 High *In-situ* Stresses

Anomalously high *in-situ* stresses, such as may be found in the vicinity of salt domes, near faults, or in the inner limbs of a fold may give rise to wellbore instability. Stress concentrations may also occur in particularly stiff rocks such as quartzose sandstones or conglomerates, which

can also lead to wellbore instability. From literature [11, 12], it is quite rare to find drilling problems caused by local stress concentrations. This is because of the difficulty in estimating or measuring such *in-situ* stresses.

2.3.1.4 Mobile Formations

Mobile formations behave in a plastic manner, deforming under pressure. They squeeze into a wellbore because they are compressed by the overburden forces within the earth's crust. The deformation occurs because the mud weight is not sufficient to prevent the formation from squeezing into the wellbore. Hence, the wellbore size is decreased as shown in Figure 2.7. Such failures are usually prevalent in salty regions. By using appropriate drilling fluids and maintaining sufficient drilling fluid weight, the formations can be stabilized [12].

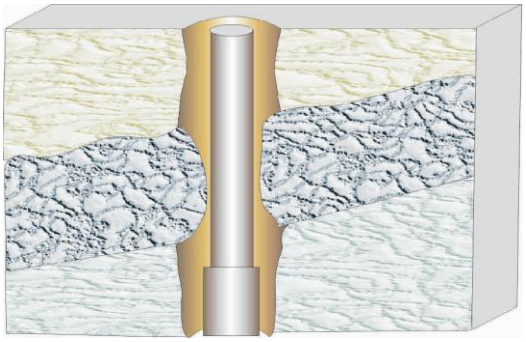

Figure 2.7: Drilling through Mobile Formations (Adapted from [12])

2.3.1.5 Unconsolidated Formations

The collapse of unconsolidated formations as their loosely packed or bounded particles, pebbles or boulders fall into the wellbore is caused by the removal of the supporting rock during drilling. When this occurs, the un-bonded formation (sand, pebbles) will no longer be supported by the hydrostatic overbalance from the fluid that flows into the formations. Hence, the sand or pebbles will fall into the hole and pack off the drill string. This instability mechanism usually occurs in shallow formations. Adequate filter cakes are usually needed to stabilize the formations [12].

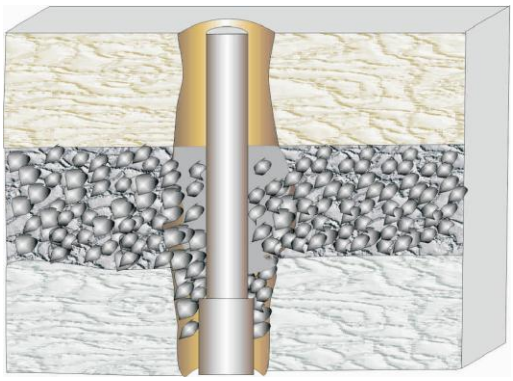

Figure 2.8: Drilling through Unconsolidated Formations (Adapted from [12])

2.3.1.6 Naturally Over-Pressurized Shale Collapse

Naturally over-pressurized shales are usually caused by geological occurrences, such as under-compaction, naturally removed overburden and uplift [12]. They have natural pore pressures that are greater than normal hydrostatic pressure gradients. By using insufficient mud weight in these formations, the drilled hole become unstable and collapse. This mechanism usually occurs in prognosed rapid depositional shale sequences and short time hole exposures as well as adequate fluid weight will help to ameliorate this problem [12].

Figure 2.9: Drilling through a Naturally Over-Pressurized Shale (Adapted from [12])

2.3.1.7 Induced Over-Pressurized Shale Collapse

Induced over-pressurized shale collapse occurs when the shale assumes the hydrostatic pressure of the wellbore fluids, after being exposed to it for a number of days. The shale then acquires a higher internal pressure than the wellbore when there is no subsequent increase or a reduction in the hydrostatic pressure within the wellbore. This leads to the shale collapsing in a similar way to naturally over-pressurized shale. This mechanism occurs in water-based drilling fluids, after a reduction in drilling fluid weight or after a long exposure time, during which the drilling fluid is unchanged [12].

Figure 2.10: Drilling through Induced Over-Pressured Shale (Adapted from [12])

2.3.2 Controllable Factors

2.3.2.1 Bottom Hole Pressure (Mud Density)

The bottom hole pressure, the mud density or the equivalent circulating density (ECD) is usually the most important factor that determines whether a wellbore is stable or not, depending upon the wellbore application. The supporting pressure provided by the static or dynamic fluid pressure during drilling, stimulation or producing of a well, determines the stress concentration around the near wellbore area. Hence, the rapidity of the fluid pressure through the wellbore will determine its stability, since rock failure is dependent on the magnitude of the effective stress around the wellbore. This is not to say that high mud densities or bottom hole pressure will always be

optimal for avoiding instabilities. For instance, in the absence of a fractured formation, high bottom hole pressure may be detrimental to stability and this can lead to formation damage, differential sticking risk, and mud hydraulics. [11]

2.3.2.2 Well Inclination and Azimuth

A significant factor that can cause hole collapse or fracture breakdown is the inclination and azimuthal orientation of a well with respect to the principal *in-situ* stresses.

This has more relevance in highly stressed anisotropy regions, such as the tectonically stressed formations. We can use these parameters to estimate the fracture breakdown pressure of the well as shown below [11, 12].

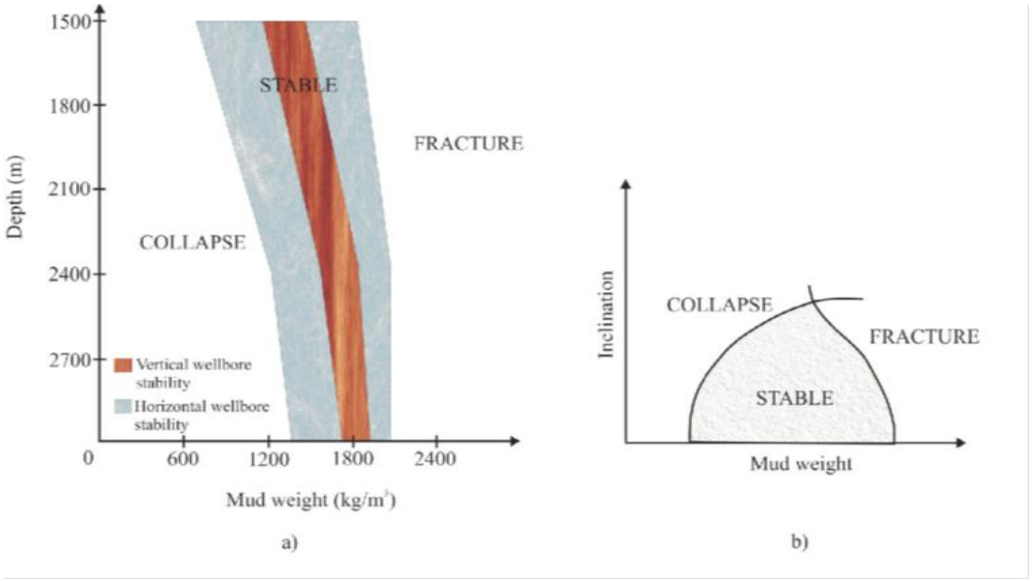

Figure 2.11: Effect of well depth (a) and the hole inclination (b) on wellbore stability (Adapted from [12])

2.3.2.3 Transient Wellbore Pressure

Transient wellbore pressures such as swab and surge effects during drilling may also cause wellbore enlargement. For instance, when the wellbore pressure across an interval is rapidly reduced by the swabbing action of the drill string, tensile spalling may occur. Also, if the formation has a very low tensile strength or is fractured, the imbalance between the pore pressures in the rock and the wellbore can cause the rock to be pulled off the wall. High

pressures can lead to rapid pore pressure increase in the near wellbore vicinity, which may cause an immediate loss in rock strength that could lead to collapse [11, 12].

2.3.2.4 Physical/Chemical Fluid-Rock Interaction

The physical/chemical fluid-rock interactions that can modify the near-wellbore rock strength or stress include; swelling, hydration, osmotic pressure, and rock softening and strength changes. The complex interaction involving many factors such as the nature of the formation (mineralogy, stiffness, strength, pore water composition, stress history, temperature), the presence of a filter cake or permeability barrier, the properties and chemical composition of the wellbore fluid, and the extent of any damage near the wellbore, all determine the magnitude of this effect [11, 12].

2.3.2.5 Drill String Vibrations (During Drilling)

In some situations, drill string vibrations may lead to the enlargement of holes. To eliminate the potential for a borehole collapse, optimal bottom hole assembly (BHA) design with respect to the hole geometry, inclination, and formations to be drilled is needed [11, 12].

2.3.2.6 Drill Fluid Temperature

Wellbore instability may arise from the thermal expansion due to high drilling fluid temperatures, or to some extent, high bottom hole producing temperatures. On the other hand, moderate/relatively low drilling fluid temperature will result in thermal contraction, and hence, prevents wellbore instability. For instance, considerable reduction of the mud temperature can cause a reduction in the near wellbore stress concentration, thereby preventing the stresses in the rock from attaining their limiting strength [11, 12].

2.4 Safe Mud Weight Window

When a wellbore is drilled, the equilibrium in-situ stress is changed. In order to support the stress relief induced by the drilling and to prevent hydrocarbon influx into the cavity, the borehole is filled with a fluid. This creates new set of stress configurations. The key point in a wellbore is to obtain the drilling fluid density that will make the wellbore stable. The lower bound to the fluid density is the collapse stress that limits shearing, while the upper bound is the fracture stress that limits the tensile failure. The fluid density between these limits is referred to as **safe mud weight window** [14]**.**

Wellbore stability during drilling centers on evaluating the drilling fluid weight to maintain the borehole integrity. It means that the pressure on the bore face must be less than formation fracture pressure and more than the pore or collapse pressure to avoid fluid losses or borehole breakouts [14]. If the drilling fluid pressure is less than the pore pressure, then formation fluid or gas may flow into the borehole, with subsequent risk of a blow out at the surface or underground. Therefore, successful drilling requires that the drilling fluid pressure lies within a safe mud-weight window defined by the drilling fluid pressure or density limits for wellbore stability [7]. This mud weight window is usually taken as the difference between a minimum and maximum weight of the drilling fluid. The wider the window, the easier it is to drill [6]. Below in Figure 2.12 is a schematic illustration of a safe mud weight window.

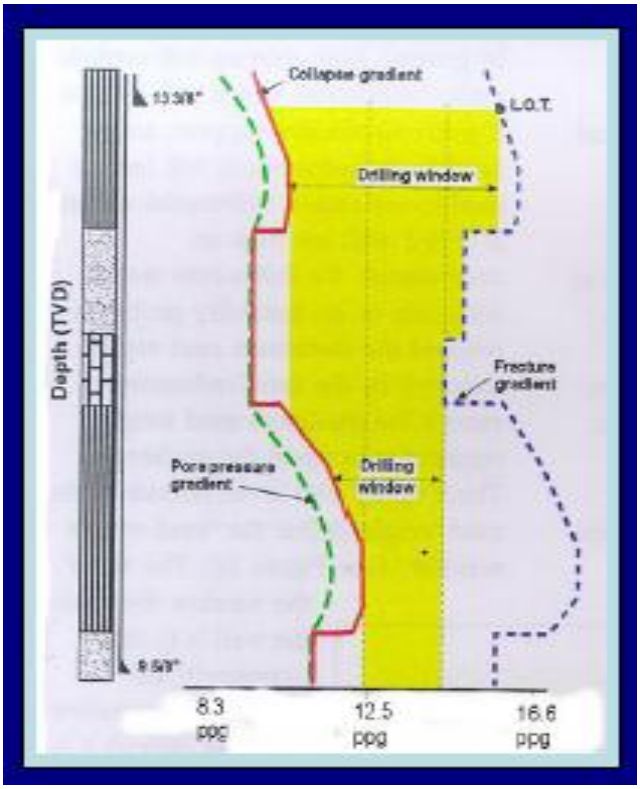

Figure 2.12: Schematic Illustration of a Typical Safe Mud Weight Window (Adapted from [6])

Typically, a safe mud weight is computed so that $P_p < P_w < \sigma_h$, where P_p is the formation pressure, P_w is the drilling fluid pressure, and σ_h is the minimum horizontal stress.

A borehole is considered "stable" when the mud weight is such that no shear or tensile failure develops. One of the ways to compute the stable mud weight window is to determine the stresses around the borehole first, and then use certain failure criteria to compare the stress state at the borehole wall with the rock strength [7].

2.5 Prediction Models for Wellbore Stability Analysis

The purpose of wellbore stability modeling is to create a safe operating window of annular pressure (mud pressure or mud weight) such that the designed fluid density will be high enough to ensure wellbore stability and low enough that fluid losses do not occur [10]. Conventionally, prediction models for wellbore stability analysis are based on rock mechanics models. The first model was proposed by Bradley in 1979 [15]. Several other mechanics-based models based have also been developed. The assumption of these models varies from simple elastic models to more elaborated elastic-plastic models [14]. These models are collectively referred to as analytical and semi-analytical models. There are also numerical models, which involve the use of finite element (FEM), finite difference (FDM), boundary element (BEM), and discrete element methods (DEM) [11, 16]. Geomechanical models and laboratory model analogues, which include thick walled cylinders and borehole collapse tests, are also used for assessing wellbore stability [11].

2.5.1 Analytical and Semi-Analytical Models

2.5.1.1 Linear Elastic Constitutive Models

The simplest models calculate the stress state at the borehole wall assuming the rock is linear elastic, homogenous and an isotropic continuum. The computed stresses are then compared to a rock strength criterion to determine whether shear failure or tensile fracture will occur (e.g., Bradley) [15, 17]. Morita also proposed an analytical procedure based on elasticity to evaluate the stress state around the borehole [18]. The stress level is compared to a compression or tensile failure criteria to evaluate stability [14]. The compression or shear failure criteria mostly used are the Mohr–Coulomb [8], Drucker-Prager [19], Modified Lade criterion [20], and Hoek and Brown [21, 22], while the tensile criterion usually compares the minimum effective stress to the tensile strength of the rock.

Linear elastic models are popular because they are relatively easy to implement, and require a modest number of input parameters compared to complex models that have a lot of input parameters, many of which cannot be realistically determined in field cases. Also, they are capable of assessing borehole instability risks for most well trajectories [17, 19]. However, these models are considered to be very conservative, since attaining the limit stress in a point around the borehole does not imply instability [15]. Models based on linear elasticity do not adequately explain the fact that, in many cases, boreholes remain stable even if the stress concentration around the borehole exceeds the strength of the formation. One way to compensate for this effect is to implement a calibration factor that corrects model predictions to match observed field data. Alternatively, elastoplastic models may also be used [17].

2.5.1.2 Elastic-Plastic Constitutive Models

Elastic-plastic models offer the ability to assess the mechanical integrity of a borehole more realistically because they incorporate the plastic behavior of the borehole. These models recognize that, even after a rock has been stressed beyond its peak strength level, it does not necessarily fail completely and detach from the borehole wall [17]. The models depend on realistic constitutive models that are able to reproduce the several failure modes around the boreholes [14]. Several authors have published analytical or semi-analytical elastic-plastic models that can account for effects such as near-wellbore, steady-state pore pressure gradients [19, 23], anisotropic in-situ stresses [24], filter-cake and capillary threshold pressures [25], and transient pore pressure gradients [26]. The challenging issue with these models is that they require a long list of input parameters, many of which have to be determined through complicated and difficult laboratory testing [3]. Some of the input parameters cannot be realistically determined in field cases [19]. Also, the test results obtained may be difficult to interpret and compare with drilling data [3].

2.5.1.3 Borehole Failure Criteria

Based on the rock strength and *in-situ* stress magnitude and directions, large stress deviations between formation and near-wellbore area may exist when a hole-wall is created by drilling. If these deviations exceed the failure criteria of a specific rock, that rock fails. Such condition may be referred to as **borehole failure.** Hence, borehole failure criteria define the boundary conditions in which the borehole failure occurs [8].

In relation to mechanical instability, there are two types of borehole failures that may occur in a rock formation as a result of increased stresses around the borehole. These include tensile failure (fracturing of the rock formation), which occurs when the pressure inside the borehole is increased to high levels, and compressive or shear failure, which occurs when the pressure is reduced to low levels that can lead to the collapse of the borehole [8, 9].

In order to tackle wellbore instability, we can determine the stresses around the borehole using the constitutive models and then compare the computed stresses with the rock formation strengths, using certain borehole failure criteria to determine whether tensile or shear failure will occur. The most commonly used failure criteria include; Mohr-Coulomb [8], Drucker-Prager [19], Modified Lade criterion [20], and Hoek and Brown [21, 22] to determine shear failure, and Maximum Tensile Stress criteria to determine tensile failure [7, 9].

Mohr-Coulomb Criterion: This is one of the most widely used shear-failure criterion that is used to evaluate the onset of borehole collapse. The model neglects the intermediate principal stresses but includes the effect of directional strengths of shales [8]. The shear-failure criterion can be expressed as [4, 8]:

$$\boldsymbol{\tau = S_o + \sigma' tan\, \alpha} \tag{2.1}$$

where, the respective axial and shear strengths are given by;

$$\boldsymbol{\sigma' = \frac{1}{2}(\sigma_1 + \sigma_3) - \frac{1}{2}(\sigma_1 + \sigma_3) sin\, \alpha - p_{fm}} \tag{2.2}$$

$$\boldsymbol{\tau = \frac{1}{2}(\sigma_1 - \sigma_3) cos\, \alpha} \tag{2.3}$$

$\boldsymbol{S_o}$, is the cohesive strength, tan $\boldsymbol{\alpha}$ is the rock coefficient of internal friction (dimensionless), σ_1 and σ_3 are the maximum and minimum horizontal principal stress respectively, α is the internal friction angle in radians, p_{fm} is the pressure of the rock formation (pore pressure), σ' is the effective stress (total compressive stress – pore pressure) and τ *is the* shear stress.

For complex stress states, such as exist at the wall of a wellbore, a number of different failure criteria have been proposed for generalizing Eq. 2.1. However, all the criteria are related to the parameters $\mathbf{S_0}$, and $\boldsymbol{\alpha}$. The Mohr-Coulomb shear failure criterion can be written as [4]:

$$\frac{(\sigma_1-\sigma_3)}{2} = S_0 cos\alpha + \frac{(\sigma_1+\sigma_3)}{2} sin\alpha \quad (2.1b)$$

where, $\frac{(\sigma_1-\sigma_3)}{2}$ is the Mohr Coulomb shear strength parameter, and $\frac{(\sigma_1+\sigma_3)}{2}$ is the average effective stress, and $\boldsymbol{\sigma_1}$and $\boldsymbol{\sigma_3}$are the maximum and minimum effective compressive stresses, respectively.

The Mohr –Coulomb equation may also be expressed in terms of the principal stresses as shown below [27]:

$$\sigma_1 = \frac{1+sin\emptyset}{1-sin\emptyset}\sigma_3 + \mathbf{UCS} \quad (2.1c)$$

where UCS is the uniaxial compressive stress and σ_1 , and σ_3, have their usual meaning.

Drucker-Prager Criterion: The Drucker-Prager criterion for shear failure combines the Mohr-Coulomb and Von Mises criteria [8]. This is why it is also known as linear extended Von Mises Criterion [20]. The criteria can be expressed, using principal stresses, as follows:

$$\tau_{oct} = \tau_o + m(\sigma_{oct} - p_{fm}) \quad (2.4)$$

where,

$$\tau_{oct} = \frac{1}{3}\sqrt{[(\sigma_1-\sigma_2)^2 + (\sigma_2-\sigma_3)^2 + (\sigma_3-\sigma_1)^2]} \quad (2.5)$$

$$\sigma_{oct} = \frac{1}{3}(\sigma_1+\sigma_2+\sigma_3) \quad (2.6)$$

σ_1, σ_2, and σ_3 are the maximum, intermediate and minimum horizontal principal stress respectively, P_{fm} is the formation pore pressure at the wellbore wall, τ_{oct}, is the octahedral shear stress and σ_{oct} is the octahedral normal stress, and τ_o and m, are Drucker-Prager strength parameters [16].

It can be shown that the relationship between the outer Drucker-Prager circle and Mohr-Coulomb criteria is expressed by:

$$\mathbf{m} = \frac{2\sqrt{2}\,sin\alpha}{3-sin\alpha} \text{ and } \tau_o = \frac{2\sqrt{2}\,S_o\,Cos\alpha}{3-sin\alpha} \tag{2.7}$$

McLean and Addis [19] reviewed the Mohr-Coulomb and Drucker-Prager failure criteria. Drucker-Prager criteria alone consist of three options, which are the inner, middle and outer circles. From their work, they concluded that among the three options of Drucker-Prager, the outer circle option is considered to produce the most realistic result of collapse pressure prediction. However, between the Mohr-Coulomb and the Drucker-Prager criteria, the Mohr-Coulomb criterion is more realistic, although the former produces a rather conservative outcome. As such when coupled with a linear elastic model, it will not give reliable predictions of minimum weight required in the field.

Modified Lade Criterion: The two failure criteria that have been discussed represent the two extreme treatments of the intermediate principal stress. The Mohr-Coulomb criterion assumes that the intermediate principal stress has zero influence on rock strength, while the Drucker-Prager Criterion gives as much weight to the intermediate principal stress as it does to the major and minor principal stresses. Under general stress states, the Mohr-Coulomb criterion will underestimate the rock strength, while Drucker-Prager criterion will overestimate it. However, the modified Lade criterion correctly accounts for the influence of the intermediate principal stress on rock strength, and therefore on wellbore stability. This criterion predicts the critical mud weight values that are less conservative than those predicted by the Mohr-Coulomb, yet are not as un-conservative as those predicted by Drucker-Prager criterion [7, 21]. The modified Lade criterion is expressed as;

$$\frac{(\mathbf{I''_1})^3}{\mathbf{I''_3}} = \mathbf{27 + \eta} \tag{2.8}$$

where,

$$\mathbf{I''_1} = (\boldsymbol{\sigma_1 + S_1 - P_o}) + (\boldsymbol{\sigma_2 + S_1 - P_o}) + (\boldsymbol{\sigma_3 + S_1 - P_o}) \tag{2.9}$$

$$\mathbf{I''_3} = (\boldsymbol{\sigma_1 + S_1 - P_o})(\boldsymbol{\sigma_2 + S_1 - P_o})(\boldsymbol{\sigma_3 + S_1 - P_o}) \tag{2.10}$$

S_1 and η are material constants, and P_o is formation pore pressure. I''_1, and I''_3 are modified first and third stress invariant. The parameter S_1 is related to the cohesion of the rock, while the parameter η represents the internal friction. Calculations show that these parameters can be directly derived from the Mohr-Coulomb cohesive strength, S_o, and friction angle, α, by:

$$\mathbf{S_1 = S_o / \tan \alpha} \tag{2.11}$$

$$\mathbf{\eta = 4 \tan^2 \alpha (9 - 7 \sin \alpha)(1 - \sin \alpha)} \tag{2.12}$$

where S_o and α are determined from triaxial compression tests.

The modified Lade criterion requires only two rock strength parameters, i.e., the cohesive strength and friction angle. It can be rearranged to obtain a closed-form solution for critical mud weight that is applicable to all wellbore orientations and in-situ stress states. Morever, it reveals that the required increase in mud weight when going from low hole angle to high hole angle is not as great as predicted by either the Mohr-Coulomb or Drucker-Prager criterion. This is due to the influence of the intermediate principal stress that is accounted for in its criterion [20].

Hoek and Brown Criterion: This criterion relates the major effective principal stress of the rock at failure (σ'_{max}) to the least effective confining stress (σ'_3). It is defined by the following relationship [21, 22]:

$$\mathbf{(\sigma'_{max}) = \sigma'_3 + \sqrt{[I_m S_c \sigma'_3 + I_m S^2{}_c\,]}} \tag{2.13}$$

where, S_c is uniaxial compressive strength, I_m is the frictional index, I_s is the intact index. These parameters define the failure envelop for the rock and are obtained by testing representative samples of materials under axial and triaxial conditions. The non-linearity and proven adequacy of this criteria in predicting observed rock fracture behavior gives the Hoek and Brown failure criteria an added advantage over that of Mohr-Coulomb on the applicable stress range of importance in wellbore stability computations [9].

Tensile Failure Criterion: Tensile failure occurs when the stress imposed by the drilling mud exceeds the tensile strength of the formation, creating a hydraulic fracture of the formation and

triggering massive loss circulation and matrix deformation. As such, this failure becomes the upper limit of the mud density window for safe drilling operations [8].

Typically, this failure occurs when the least effective principal stress exceeds the formation rock tensile strength [8, 12, 28]. We can express this criterion as:

$$\boldsymbol{\sigma'_3 \leq \sigma_f} \tag{2.14}$$

where $\boldsymbol{\sigma_f}$ is the tensile strength of the formation rock, and the least effective principal stress is given by least total stress minus the pore pressure, i.e.

$$\boldsymbol{\sigma'_3 = \sigma_3 - P_f} \tag{2.15}$$

2.5.2 Geomechanical Models

Geomechanics plays a significant role in assessing the stability of a wellbore during drilling. Through it, we can obtain a safe mud weight window that can be used to drill a well with minimum damages and improved turnaround time. In order to build a geomechanical model or simulator for the formation of interest, several sets of data are needed as inputs. These data include: rock mechanical properties measured in the lab on core samples and field measured data such as logs and directly measured in situ stresses [29]. Table 2.3 summarizes some sources of geomechanical data [30].

Table 2.3: Geomechanical Data Sources

Input Data	Sources of Data
Vertical or Overburden Stress	Integrated density Density from sonic/seismic logs
Pore Pressure	Measurements (RFT, DST, PWD) Log-based (sonic, resistivity) Seismic (ITT, velocity cubes)
Least/ Minimum Horizontal Stress	XLOT, LOT, minifrac, lost circulation, ballooning
Maximum Horizontal Stress (Magnitude) Maximum Horizontal Stress (Orientation)	Analysis of wellbore failure Crossed dipole sonic (orientation) "Active" geological structures
Rock Strength	Core tests, logs, cuttings, analysis of wellbore failure

The stability of a wellbore is determined by integrating data, such as *in-situ* stresses (vertical and horizontal), well pressure, rock mechanical and drilling fluid properties, resulting in a comprehensive geomechanical model for wellbore stability analysis. Integration of such data leads to four main sets of inputs that describe a geomechanical model for a formation of interest. These sets are: *in-situ* stress magnitudes, *in-situ* stress directions, pore pressures and elastic properties of the rock. *In-situ* stresses include: the vertical stress or the overburden stress, minimum horizontal stress and maximum horizontal stress. The elastic properties include: the Young's modulus, Poisson's ratio, cohesion, internal friction angle, and the unconfined compressive strength of the rock. Other elastic properties such as bulk modulus and shear modulus can be derived from these sets of parameters [29].

A geomechanical approach was used to optimize the drilling and completion strategy of an unconsolidated sandstone reservoir in Saudi Arabia. The model enabled certain results to be obtained that led to the discovery of how to maximize borehole stability and minimize required mud weights during drilling and completion of the undepleted horizontal wells in the Saudi Arabian oil fields [31]. Also, Mohiuddin et al. [32] used a geomechanical stimulator (known as Pbore-3D) with field data as input to predict the safe mud weight window for some horizontal

wells in Saudi Arabia. Al-wardy et al [29] were able to develop a geomechanical model for wellbore stability during drilling through the Nahr Umr Shales in an Oman oilfield. Considering the cited cases, geomechanical models have been successfully used to assess wellbore stability. However, the problem is that rigorous analyses that have to be carried out in order to obtain the relevant data to be used in developing the model [30]. This remains an unresolved challenge in the oil and gas industry.

2.5.3 Numerical Models

Numerical models discretize the wellbore instability problems into smaller elements and then you solve them using techniques such as finite element (FEM), finite difference (FDM), boundary element (BEM), and discrete element methods [11]. These models, which are often used to simulate the effects of plastic deformation, present the advantage of showing the extent of the damaged region, leading to a better indicator of instability. More so, these models usually consider two kinds of failure around the wellbore: shear failure and tensile failure [14].

A numerical technique, such as finite element method has been used to solve wellbore stability boundary value problems associated with an elastoplastic constitutive model [16]. Zahn et al [14] considered the stability of oil wells by under volumetric compressive deformation around the borehole. They were able to model the borehole instability phenomena by using a numerical model that was implemented with the aid of a commercial ANSYS finite element code. As well, for advanced borehole stability modeling, a number of numerical geomechanical models can be used. These models are capable of very realistic representations of rock deformation, yielding and fluid flow behavior. However, these numerical models are very expensive to execute. They require expert users to run the codes. The computational times are also lengthy, with numerous input parameters required [17]. These models have become even more complex as they incorporate more of the physics associated with instability. These include: poroelasticity [33], thermoporoelasticity [34], and chemo-thermoporoelasticity [35, 36].

2.6 Previous Studies on Wellbore Stability

Over the past decade, substantial contributions have been made towards the successful drilling of hydrocarbon wells in the oil and gas industry. A borehole stability analysis was carried out (by Fuh et al., 1991) [37]. Before the drilling of the first horizontal well drilled in Block K/18 of the Dutch Sector of the North Sea Field, data from previous eight vertical wells drilled in the area were analyzed and used to construct a geomechanic model that simulated the potential behavior of the horizontal well under design. The challenge was to drill a high-angle hole through the highly reactive and potentially over-pressured Vlieland Shale, then into the partially depleted underlying Vlieland Sandstone. Borehole stability analysis provided useful information for the drilling of the horizontal well with few manageable problems of instability.

In 1992, Santarelli et al., [38] presented a case study of drilling in highly fractured volcanic rocks at great depths. It was found that the main mechanism of instability was mud penetration in fractures that led to the eventual erosion of the wellbore wall due to inadequate wall support. By simulating the fractured rock mass using discrete element modeling (DEM), an appropriate mud weight was obtained. The use of this new mud weight proved successful.

Ong and Roegiers, 1993 [39] presented an anisotropic model for calculating the stress around wellbore. They concluded that the borehole collapse is a manifestation of shear failure, which in a horizontal wellbore, is significantly affected by high degrees of rock anisotropy, high *in-situ* stress anisotropy, and excessive cooling of the wellbore. According to Ong and Roegiers, pore pressure and porous elastic constant also affect the shear failure though the effect is less pronounced.

Morita and Ross, 1993 [40] described a new core-based well stability analysis for horizontal or highly inclined wells in weak formations. New procedures to measure core strength and deformation, and the numerical procedure to calculate the well stability for a highly non-linear formation were presented in their work. They concluded that the core-based borehole stability analysis gives a reliable safe mud range for both weak sands and shale zones, but cautioned that a linear model should not be used for the analysis except it is used as a base function of a functional interpolation or extrapolation technique.

Wong et al., 1994 [41] proposed thick-walled-cylinder strength tests (TWC) that involved taking cores. Their method was used in deriving the necessary mechanical data used in borehole stability analysis for drilling horizontal well in the North Sea. Based on their study, the elastic/brittle model prediction was shown to be unrealistically conservative. Nevertheless, the model qualitatively indicates the solution's sensitivity to different field input parameters. According to the authors, the TWC empirical approach is a new, simple method that provides a quick, qualitative borehole stability assessment. Elastoplastic analysis gives a realistic mud weight prediction, but it is the most expensive test to perform.

In 1991, lost time due to stuck pipe related drilling problems accounted for approximately 18 % of total drilling time in Mobil Producing Nigeria (MPN) offshore operations. The primary cause of stuck pipe was identified as mechanical wellbore instability. In order to solve this problem, Lowrey and Ottesen, 1995 [9] reported that MPN has to carry out borehole stability study and the result was productive. Data acquisition involved taking conventional cores in the zone of interest, which can make the cost of borehole stability study unattractive. The parameters obtained were used to perform a geometrical simulation and estimate safe mud weights. Use of these mud weights led to a marked improvement in wellbore stability.

Marisela et al., 1996 [42] used borehole stability 2-D model to analyze the borehole condition under open hole completion in Venezuela. A 2-D finite element model was developed with a generalized plasticity constitutive equation. A safe drawdown to prevent failure was determined and the well was completed under open hole without any production liner. The well produced above the estimated potential without any sanding or stability problems.

Santarelli et al., 1996 [43] presented wellbore instability problems occurring in a developed field in Italy. The problems were analyzed with respect to the mud weights, mud types, stress regime and azimuths. Based on the data obtained, drilling operations were successfully carried out with necessary modifications.

Cui et al., 1999 [44] developed a software PBORE-3D for windows which is capable of performing stability analyses of boreholes. The model considers the fully coupled effects between the rock matrix and the pore fluid using recently-developed poroelastic borehole

models. PBORE-3D was used to analyze stress/pore pressure, formation failure, and mud weight design.

Fung et al., 1999 [45] also developed a finite element elasto-plastic model that can perform effective stress analysis of the near wellbore tensile and shear failure. Their model has the capability of handling extremely low confining stresses in unconsolidated formations, as plastic yielding occurs at relatively low deviatoric confining stress conditions, which is not a good indication of wellbore failure in terms of loss of service. They, therefore, developed a more realistic criterion based on the accumulated plastic strain. The model was successfully used to analyze the stability of two horizontal wells with open-hole completions in unconsolidated oil sand.

For modeling naturally fractured reservoirs, Zhang and Roegiers, 2000 [46], developed a dual porosity poroelastic model that is effective and accurate in the characterization of stresses and flow fields. They also developed a generalized plane strain and dual porosity finite element solution for analyzing horizontal borehole stability. Their results show that horizontal borehole stability depends strongly on the *in-situ* stress state, the borehole orientation, time, drilling fluid pressure and fracture characteristics.

Finkbeiner et al., 2000 [47] presented a case study of drilling and completing horizontal well in the shallow unconsolidated oil field of California. The evaluation of rock strength and the tectonic stress revealed that the maximum horizontal stress was greater than the overburden stress. Maximum horizontal compression was oriented N60^{o}E. The borehole stability of the horizontal well was predominantly controlled by the extremely weak reservoir rock. Through the borehole stability analysis, they predicted borehole collapse during production for open hole completion. The borehole stability analysis was also used to select the type of completion (60 mesh slotted liner) and the horizontal well produced successfully without sand problem.

Saidin and Smith, 2000 [48] discussed wellbore instability encountered when drilling through the Terengganu shale (K-shale) in the Bekok field in Malaysia. Due to the time dependency of the observed instability cases, K-shale was thought to be reactive and unstable due to shale-fluid interactions. But after rock characterization and lab measurements of rock mechanical properties were carried out, the results showed that K-shale had predominantly non-reactive weak clay.

This information helped to improve the design of the mud weight window, which led to the successful completion of a new well.

Severe instability was encountered while some drilling horizontal drains in Hamlah-Gulailah formation, ABK field, offshore Abu Dhabi. In analyzing the instability problem, Onaisi et al., 2000 [49] reported that a comprehensive rock mechanical study was carried out to characterize the rock strength and *in-situ* horizontal stresses. The study suggested that the horizontal stresses were anisotropic in nature with strike-slip-thrust stress regimes. The rock mechanical simulation predicted higher mud weights than those actually used in the field.

Morita 2004 [18] presented a study on "Well Orientation Effect on Borehole Stability". It was concluded that actual rocks are not linear elastic materials. Before a borehole collapse, the non-linearity of the rock deformation becomes significant. The significant non-linearity reduces the stress concentrations induced by directional *in-situ* loads. In addition, an oriented borehole has a non-uniform stress or stress gradient around a borehole. The stress gradient reduces the stress concentration area. Since the smaller size of the stress concentrated region is less liable to fail then the well bore stability is mostly controlled by the maximum radial stress after local failures, rather than the ratio of the radial principal stresses.

Simangunsong et al., 2006 [8] reported that depending on the source of the problem, wellbore instability is classified either as mechanical or chemical. Chemical wellbore instability, often called shale instability, is most commonly associated with water adsorption in shaly formations, where the water phase is present and can cause borehole collapse. In contrast, mechanical wellbore instability is caused by applying mud of insufficient weight, which will create higher hoop stresses around the hole-wall. Hoop stresses around the hole-wall are often excessively high and result in rock failure. The most rapid remedy for this instability is to increase mud weight and/or adjust the well trajectory for high-angle wells. The mechanical instability occurs as soon as the new formation is drilled, but chemical instability is time dependent because shales are subject to strength alteration once exposed to different drilling fluids. A series of experimental studies led to the conclusion that shale strength decreases with time, when the shale is exposed to most drilling fluids. Despite the tendency of shale to experience chemical instability, it can also experience mechanical instability simultaneously, which can lead to a more complex problem.

Mody et al., 2007 [50] presented the need for a sustainable deployment of geomechanics technology to reducing well construction costs. The major hurdles in borehole stability studies currently are often due to, but not limited to, the following factors:

1. The majority of easily accessible oil and gas reservoirs have already been exploited. The trend in hydrocarbon exploration is steadily moving to deeper and more complex environments (e. g., in deep water, sub-salt high pressure high temperature (HPHT) and other challenging environments);
2. Data regarding rock mechanical properties, in-situ stress states and geological structures cannot be accurately defined and are often provided with large uncertainties;
3. Well engineers, petro physicists and drillers who are directly involved in well delivery may not have adequate time and training in identifying and managing borehole instability issues;
4. Due to lack of resources and time constraints, well operations after action reviews typically gets lower priority and as a consequence, these reviews may not be well documented.

Mody et al., [50] also stated that borehole stability related downtime associated with well construction is typically 10-15 % of the total well cost and about 50 % of total non-productive time.

Drilling horizontal wells, single and multilateral, is a common practice for Saudi Aramco. For effective drilling and reservoir management, a borehole stability study was carried out by Raba'a et al., 2007 [31]. This was used to identify the optimum mud weight and well azimuth to place long reach horizontal wells, so as to minimize the risk of stress-induced borehole breakouts. Also, to optimize drilling mud weights and to aid in making informed decisions about adequate completions designs, as well as ensure sustainable production under depletion modes. They concluded that under undepleted conditions, horizontal wells should be drilled with oil-based mud, parallel to the field-derived maximum principal horizontal stress azimuth, in order to maximize borehole stability and minimize required mud weights during drilling and completion.

Sinha et al., 2008 [51] presented an algorithm on how to estimate the rock stresses from borehole sonic data. Their work was only for sand reservoirs. However, the borehole stability problems occur in shale.

Nguyen and Abousleiman, 2009 [52] developed an analytical porochemothermoelastic solution for an inclined wellbore that coupled transient chemical and thermal effects on shale stability. The shale was modeled as an imperfect semi-permeable membrane which allows partial transport of solutes. In addition to chemical osmosis, both solute transport and thermal effects were taken into account to realistically model field conditions.

Furul et al., 2009 [53] used the borehole stability analysis approach to investigate the causes of production liner deformation for inclined/horizontal wells completed in a highly compacting chalk formation. Based on the review of historical caliper survey data, they ascertained that the axial compression collapse is a major liner deformation mechanism in the reservoir zones. Axial compression collapse has been found in both low-angle wells (also buildup sections of horizontal wells) and horizontal laterals. The casing deformation in low-angle section are due to reservoir compaction (i.e., change in the vertical formation strain), while the deformation in horizontal sections are primarily induced by increased axial loading due to cavity deformation. The completion practice using cluster perforations and high volume acid treatments led to vertically enlarged cavities and resulted in poor radial constraint.

Soreide et al., 2009 [54] studied the effect of anisotropy on shale borehole stability in high pressure and high temperature well. They concluded that the effect of anisotropy is most pronounced when drilling at high inclination angles, almost parallel to the bedding. A mixture of failure modes may also be observed.

Li and Purdy, 2010 [55] in their study on how to estimate maximum horizontal stress proposed two methods. The first method is based on a generalized Hooke's law, with coupling the equilibrium of three in-situ stress components and pore pressure. They believed that this new technique can reduce the uncertainty of *in-situ* stress prediction by narrowing the area of the conventional polygon of the *in-situ* stresses. The second method involves the analysis of drilling-induced near-wellbore stresses and breakouts using the Mohr-Coulomb failure criterion.

Lang et al., 2011 [10] concluded that the work flow for wellbore stability modeling should consider bedding planes, rock anisotropy and pressure depletion. With the consideration of these factors, the wellbore model enables the calculation of wellbore failures along borehole trajectories with various drilling orientations versus bedding directions. At the end of the study,

they were able to develop a wellbore stability model and real-time surveillance for the drilling operations in deep-water Gulf of Mexico. By applying this model and observing real-time updates, the drilled well reached target depths safely. It also decreased the drilling cost by 6 million dollars.

2.7 Theory of Fracture Mechanics

Fracture mechanics is defined as the field of solid mechanics that deals with the behavior of cracked bodies subjected to stresses and strains. The stresses can arise from primary applied loads or secondary self-equilibrating stress fields (e.g. residual stresses) [56]. It is also referred to as the field of mechanics concerned with the study of the propagation of cracks in materials [57]. It uses the methods of analytical solid mechanics to calculate the driving force on a crack and those of experimental solid mechanics to characterize the material's resistance to fracture [57].

Fracture mechanics can be divided into linear elastic fracture mechanics (LEFM) and elastic-plastic fracture mechanics (EPFM) [58]. LEFM is the basic theory of fracture that deals with sharp cracks in elastic bodies [59]. It assumes that the material is isotropic and linear elastic. Based on this assumption, the stress field near the crack tip is calculated using the theory of elasticity. When the stresses near the crack-tip exceed the material fracture toughness, the crack will grow. For brittle materials, it accurately establishes the criteria for catastrophic failure. In the presence of inelastic deformation, LEFM is valid only when the size of such deformation is small compared to the size of the crack (i.e., when small-scale yielding occurs) [60].

EPFM is employed when large zone of plastic deformation develops before the crack propagates, as experienced in ductile materials [58, 60]. It assumes isotropic and elastic-plastic materials. Based on this assumption, the strain energy fields or opening displacement near the crack tips are calculated. When the energy or opening exceeds the critical value, the crack will grow [60]. It should be noted that although the term elastic-plastic is commonly used in this approach, the material is merely **nonlinear- elastic** [60]. In other words, the unloading curve of the so called elastic-plastic material in EPFM follows the original curve, instead of a parallel line to the linear loading part, which is normally the case for true elastic-plastic materials. See sketches below.

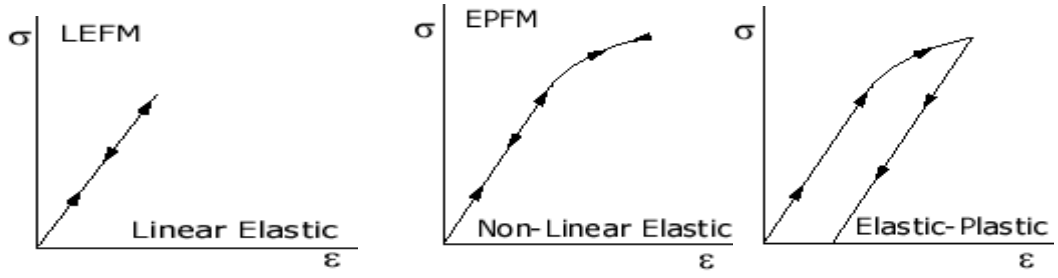

Figure 2:13: Sketches of Stress versus Strain in LEFM and EPFM (Adapted from [60])

2.7.1 Fracture and Modes of Fracture

Fracture in materials is simply defined as the separation of a body into two or more pieces in response to an imposed stress that is static (i.e., constant or slowly changing with time) and at temperatures that are low relative to the melting temperature of the material [61]. The applied stress may be tensile, compressive, shear, or torsional. For most materials, fractures can be classified into two general categories; ductile fracture and brittle fracture [62]. Any fracture process involves the following two steps: crack initiation and propagation (in response to an imposed stress) [61, 62].

Crack initiation is the process by which one or more cracks (micro-scale discontinuities), are formed in a material hitherto free from any other cracks [63]. It can occur when the material is subjected to normal stresses (as in the case of ductile fracture) [61] or as a result of thermal stresses induced within the material when subjected to heat [63]. It may also occur during manufacturing and micro-mechanical processes [63, 64]. In response to an imposed stress, the micro-scale cracks, which usually have dimensions of about (1-1000 microns) grows into meso-cracks (several hundreds of microns to a few millimeters in dimension) and then into macro-cracks (several millimeters to decimeters in dimension), in which fracture is then said to have occurred [65]. It is important to note that all materials have micro-scale discontinuities present in them. In reality, rock materials are discontinuous at all scales. At the micro-scale, defects causing stress concentrations are micro-cracks, grain boundaries, pores, and bedding planes, while at the macro-scale geological fractures are referred to as joints (opening) and faults (shearing), based on their genesis [63].

Ductile fracture is characterized by appreciable plastic deformation prior to and during the propagation of the crack. An appreciable amount of gross deformation is usually present at the

fracture surfaces, as observed in ductile materials, such as most metals [62]. On the other hand, brittle fracture occurs without any appreciable prior deformation. It also occurs by rapid crack propagation, as observed in brittle materials, such as ceramics [61]. Crack propagation may occur along low index crystallographic planes (referred to as transgranular or cleavage fracture) or along the grain boundaries of the materials (referred to as intergranular fracture) [61, 66]. Figure 2:14 shows schematic illustrations of ductile and brittle fracture in response to an applied tensile stress.

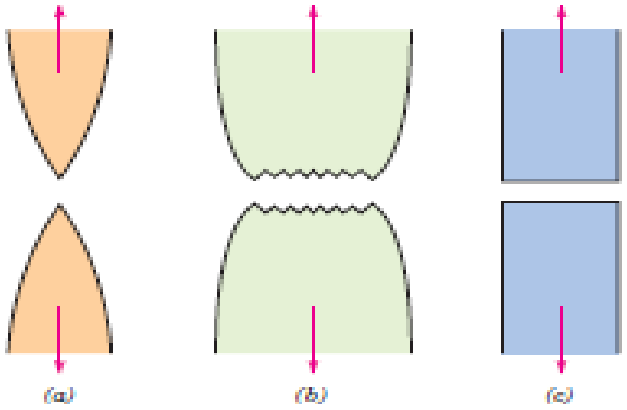

Figure 2:14: Brittle versus ductile Fracture a) Highly ductile fracture with gross plastic deformation (necking), b) Moderately ductile fracture, and c) Brittle fracture without any plastic deformation (Adapted from [61])

Fracture in materials can occur by three different modes depending on the direction of the crack propagation [66] or the crack surface displacement [65]. These modes are shown below:

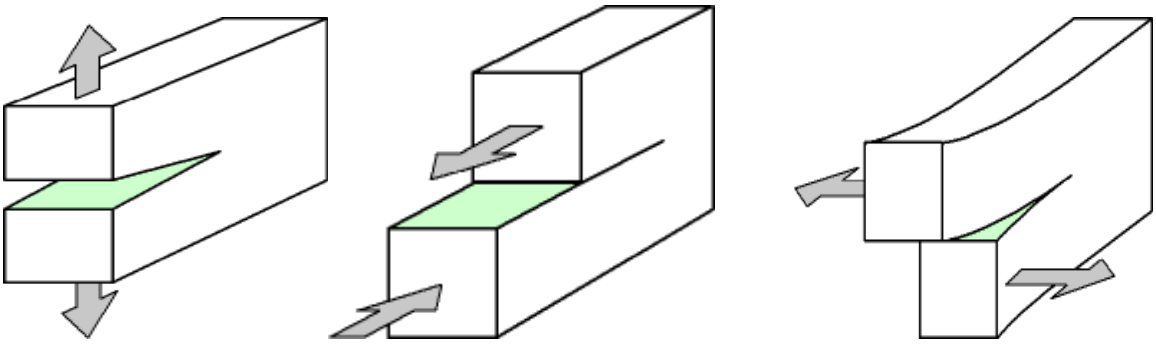

(a) Mode I **(b) Mode II** **(c) Mode III**

Figure 2:15: Modes of Fracture (Adapted from [60])

Mode I: This is generally referred to as the crack opening or tensile mode. The crack-tip is subjected to a stress normal to the crack plane, such that the crack faces separate at the crack front. As such, the displacements of the crack surfaces are perpendicular to the crack plane, while the crack propagation is along the crack plane direction. The crack carries no shear traction and no record of shear displacement is visible [63, 65]. It is often the most dangerous of all the loading modes [66].

Mode II: This is referred to as the edge sliding or in-plane shearing mode. The crack-tip is subjected to an in-plane shear, such that the crack faces slide relative to each other. This causes the displacements of the crack surfaces to be parallel to the crack plane and perpendicular to the crack front. Shear traction occurs parallel to the crack plane [63, 65].

Mode III: This is termed tearing or out-of-plane shearing mode. The crack tip is subjected to an anti-plane shear stress such that the crack faces move relative to each other. Hence, the displacements of the crack surfaces are along the crack plane but parallel to the crack front [63].

Each of these modes may occur separately or simultaneously. Any combination of the three basic modes is referred to as ***mixed mode***. The principle of superposition is sufficient to describe the most general case of crack tip deformation [65].

2.7.2 Linear Elastic Fracture Mechanics (LEFM)

LEFM is based on the elastic analysis of a cracked body. There are two basic crack driving forces that can be used to characterize linear elastic fractures. These are the strain energy release rate (G) and the stress intensity factor (K) [60]. This section presents the underlying concepts of LEFM.

2.7.2.1 Griffith Fracture analysis and Strain Energy Release Rate

In 1920, A.A. Griffith proposed that a brittle material contains numerous micro-cracks and flaws, which are distributed randomly throughout the material. The discontinuities produce stress concentration of sufficient magnitude in localized regions, which causes a significant reduction in the tensile strength of the material when compared to its theoretical cohesive strength [67]. He established the following criterion for the propagation of a crack: A crack will propagate when the decrease in elastic strain energy is at least equal to the energy required to create new crack

surfaces [67]. This criterion can be used to determine the magnitude of the tensile stress which will cause a crack of a certain size to propagate as a brittle fracture [62].

The Griffith approach is based on the stress analysis of Inglis [68] who showed that the local stresses around an elliptical hole (notch) could increase to a level several times that of the applied stresses [63]. This is expressed as:

$$K_t = \frac{\text{Maximum stress around the notch tip}}{\text{Local stress away from the notch}} = 1 + 2\sqrt{\frac{a}{\rho}} \quad (2.16)$$

where a is the notch length and ρ is the notch radius of curvature.

By considering the thermodynamic balance between the energy required to create new crack surfaces, and the change in internal (strain) energy associated with the displacement of specimen boundaries (**Figure 2.16**), Griffith was able to obtain the following energy balance equation:

$$U_T = -\frac{\pi\sigma^2 a^2 B}{E'} + 4a\gamma_s B \quad (2.17)$$

where, the first half on the right-hand side corresponds to the strain energy and the second half of the right-hand side is the surface energy due to the upper and lower faces of the crack, which have a total surface area of 4aB. Also, σ is the applied stress, a is the crack length, B is the thickness of the specimen, $E' = \frac{E}{(1-v^2)}$ for plane strain, and $E' = E$ for plane stress, where E is the Young's modulus, v is Poisson's ratio, and γ_s is the surface energy associated with the creation of the crack surfaces [66].

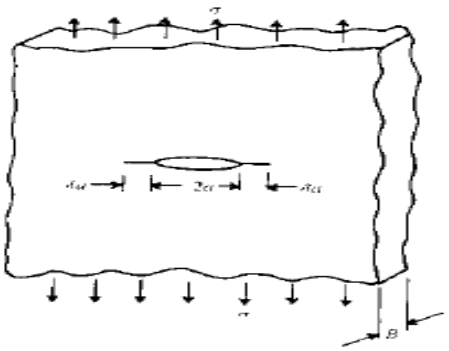

Figure 2.16: Griffith Crack: A Centre Crack of Length 2a in a large Plate Subjected to Elastic deformations (Adapted from [66])

The critical condition at the onset of unstable equilibrium is determined by equating the first derivative of Eq. 2.17 to zero, i.e., $dU_T/da = 0$. This gives:

$$\frac{dU_T}{da} = -\frac{2\pi\sigma^2 aB}{E'} + 4\gamma_s B = 0 \quad (2.18)$$

Solving the above expression, we obtain:

$$\sigma_c = \sqrt{\frac{2\gamma_s E'}{\pi a}} \quad (2.19)$$

where, σ_c is the Griffith fracture stress obtained by re-arranging Eq. (2.18), and the other terms have their usual meaning. Equation (2.19) does not account for the plastic work that is done during the fracture of most materials. It is, therefore, only applicable to very brittle materials in which no plastic work is done during crack extension.

If we rearrange the Griffith expression earlier on obtained in equation 2.19, we obtain:

$$\frac{\pi\sigma^2 a}{E'} = 2\gamma_s \quad (2.20)$$

The left-hand side of the equation represents the elastic energy per unit crack surface. This energy is available for crack propagation and it defines an important parameter called the strain energy release rate, denoted by *G* in honor of Griffith. Thus, an expression for the strain energy release rate *G* can be given by:

$$G = \frac{\pi\sigma^2 a}{E'} \quad (2.21)$$

The Griffith theory for the critical condition for fracture initiation becomes:

$$G = G_C \quad (2.22)$$

where, G_C is the critical strain energy release rate. G_C is defined as the critical value of strain energy released per unit length of crack extension. More generally, *G* is defined as the derivative of the elastic strain energy release with respect to crack area rather than crack length. The above formulation describes a simple case of a flat and open elliptical crack subjected perpendicularly to a uniaxial tensile load and it is assumed that the crack propagates along its own plane. This indicates that the strain energy release rate is the governing parameter for fracture initiation in LEFM.

In 1950, Orowan [69] modified equation 2.19 to account for plastic work in materials that undergo plastic deformation prior to catastrophic failure. He proposed the following expression for the critical fracture condition, σ_c:

$$\sigma_c = \sqrt{\frac{2(\gamma_s+\gamma_p)E'}{\pi a}} \tag{2.23}$$

where, γ_p is a plastic energy term, which is generally difficult to measure independently.

2.7.2.2 Stress Intensity Factor and Fracture Toughness

The stress intensity factor (K) can be defined as the amplitude of the crack-tip stress field around a crack or fracture in a material. More importantly, K, represents the driving force for a crack growth under LEFM conditions [66]. For each mode of fracture, K, may be defined in terms of the crack-tip stresses as follows:

$$K_I = \lim_{r\to 0}[\sqrt{2\pi r}\,\sigma_{yy}\,|\theta = 0] \tag{2.24}$$

$$K_{II} = \lim_{r\to 0}[\sqrt{2\pi r}\,\sigma_{xy}\,|\theta = 0] \tag{2.25}$$

$$K_{III} = \lim_{r\to 0}[\sqrt{2\pi r}\,\sigma_{xz}\,|\theta = 0] \tag{2.26}$$

where, $\sigma_{yy}, \sigma_{yy}, \sigma_{yy}$ are crack-tip stresses in the yy, xy, and xz directions of the crack plane and r is the radial distance from the crack tip.

In a general form, the stress intensity factor, K , is expressed as:

$$K = f(a/w)\sigma\sqrt{\pi a} \quad (2.27)$$

where, σ is the applied stress, f (a/w) is a function of the crack length, a, and width, w, of the specimen. For an edge crack in a semi-infinite body, f (a/w) = 1.12 and for a crack in an infinite body, f (a/w) = 1. Wang, 1996 [58] presented the geometry functions of different fracture mechanics geometries. This could be a helpful guide for more complex geometries.

The fracture toughness (K_C) is basically a property of the material reflecting its resistance to physical macroscopic separation through crack propagation [63]. Conceptually, K_C is a constant and should not vary with various factors. Fracture initiation occurs when the stress intensity (K) factor reaches a critical value, which is the fracture toughness, K_C:

$$K = K_C \quad (2.28)$$

It follows from equation 2.28 that for Mode I fracture, fracture initiation, which refers to the propagation of pre-existing cracks, will occur when the stress intensity factor of the Mode I fracture, $K_{I,}$ reaches a critical value, called the Mode I plane strain fracture toughness, K_{Ic}:

$$K_I = K_{Ic} \quad (2.29)$$

Similarly, in Mode II, when the crack tip stress intensity factor, K_{II}, reaches the Mode II fracture toughness, K_{IIc}, the crack will propagate. Same concept also applies for Mode III fracture.

Analyses related to Mixed-mode loading conditions are common. For example, for an angled (inclined) crack subjected to a uniform far-field compressive stress, both K_I and K_{II} modes at the crack tip must be considered. According to the superposition principle, the crack tip stress and displacement components can be obtained by superimposing those resulting from pure Mode I and pure Mode II loadings. Fracture initiation will occur when a certain combination of K_I and K_{II}, f ($K_{I,}$ K_{II}), reaches a critical value, f $(K_{I,} K_{II})_c$. The quantity f $(K_{I,} K_{II})_c$ is known as the Mixed-mode I-II fracture toughness envelope or the $K_{I,}$ K_{II} envelope [63].

2.7.2.3 Equivalence of G and K

In 1957, Irwin [70] proposed the relationship between the strain energy release rate, G, which is the global energy parameter and the stress intensity factor, K, which is local crack tip stress field parameter for the three modes of fracture, as shown below:

$$G_I = \frac{K_I^2}{E'} \tag{2.30}$$

$$G_{II} = \frac{K_{II}^2}{E'} \tag{2.31}$$

$$G_{III} = \frac{K_{III}^2}{2\mu} \tag{2.32}$$

where, G_I, G_{II}, and G_{III} are the strain energy release rates for Mode I, Mode II, and Mode II, respectively, $\mu = E/2(1+v)$, $E' = \frac{E}{(1-v^2)}$ for plane strain, and $E' = E$ for plane stress, where E is the Young's modulus, and v is Poisson's ratio.

The above relations between G and K for different modes of loading are obtained by assuming that the crack extends along its own plane. If a crack extends at an angle with respect to the crack plane, the relation between G and K is more complex. When a crack is exposed to a mixed-mode I-II loading, the overall strain energy release rate, G, is a summation of the Mode I strain energy release rate, G_I, and that of Mode II, G_{II}, which indicates that the strain energy release rates for various loading modes are additive and that the superposition principle applies not only to the same mode but also for different modes. This is similar to the crack tip stress and displacement fields, but is unlike the stress intensity factors that are additive only for the same mode [63].

2.7.3 Elastic-Plastic Fracture Mechanics (EPFM)

EPFM is based on the theory of elastic-plasticity. There are two major parameters used in evaluating EPFM. These are the crack tip opening displacement (CTOD) suggested independently by Wells [71] and Cottrell [72], popular in Europe, the J-integral proposed by Rice and Rosengren [73], widely used in the United States. These parameters are valid in

characterizing crack tip toughness for elastic-plastic materials. The basic EPFM analysis can be summarized as follows:

1. Calculate the J integral or crack tip opening displacement (CTOD) as a function of the loading and the geometry.

2. The critical J integral, J_C, or the critical CTOD, δ_C, can be determined empirically.

3. The J integral J should NOT exceed J_C, or, the CTOD should not exceed the critical CTOD, δ_C.

2.7.3.1 J Integral: J integral is defined as [65];

$$J = \int_{\Gamma} \left(Wdy - T\frac{du}{dx}ds\right) \tag{2.33}$$

where W is the strain energy density, which is given by:

$$W = W(x, y) = W(\varepsilon) = \int_0^{\varepsilon} \sigma_{ij} d\varepsilon_{ij} \tag{2.34}$$

where Γ is an arbitrary closed contour around the tip of the crack, T is the traction perpendicular to Γ, ds is an element of Γ, σ, ε, and *u* are the stress, strain, and displacement field, respectively.

Rice et al. 1968 [73], showed that the J integral is a *path-independent* line integral and it represents the *strain energy release rate of nonlinear elastic materials*:

$$J = -\frac{1}{B}\frac{d\Pi}{da} \tag{2.35}$$

where $\Pi = U - W$ is the potential energy, the strain energy U stored in the body minus the work W done by external forces, da is the crack extension and B is the thickness of the specimen.

For *linear elastic* materials, $-\frac{1}{B}\frac{d\Pi}{da} = G$, which means that J = G for the linear elastic case. Also under small scale yielding, J is uniquely related to stress intensity factor, K as follows:

$$J = G = \frac{K^2}{E'} \tag{2.36}$$

where E' = E for plane stress, $E' = \frac{E}{(1-v^2)}$ for plane strain, and v is Poisson's ratio.

2.7.3.2 The Crack Tip Opening Displacement (CTOD): The two most common definitions of CTOD are [59]:

1. The displacement at the original crack tip.

2. The so called 90^0 intercept.

The above two definitions are equivalent if the crack blunt is semicircle.

For plane stress conditions, CTOD, $\delta = \frac{K^2}{E\sigma_{ys}}$ (2.37)

For plane strain conditions, CTOD, $\delta = \frac{K^2}{2E\sigma_{ys}}$ (2.38)

where σ_{ys} is the small scale yielding stress, E is the Young's modulus and K is the stress intensity factor.

We can obtain a relationship between J and CTOD if we consider a linear elastic body containing a crack, the J integral and the crack tip opening displacement (CTOD) will be as follows [60]:

$$J = \frac{K^2}{E} = m\sigma_{ys}\delta \tag{2.39}$$

where m is a dimensionless constant that depends on the material properties and stress states. For plane stress and non-hardening materials, m = 1. Hence, for a through crack in an infinite plate subjected to a remote tensile stress σ (Mode I), the crack tip opening displacement, δ, is

$$\delta = \frac{K_I^2}{E\sigma_{ys}} = \frac{\pi a\sigma^2}{E\sigma_y} = \frac{G}{\sigma_y} = \frac{J}{\sigma_y} \tag{2.40}$$

2.8 References

[1] Aadnoy, B., "Modeling of the Stability of Highly Inclined Boreholes in Anisotropic Rock Formations", *SPE Drilling Engineering*, p 259, September, 1988

[2] Osisanya, S. O., and M. E. Chenevert., "Physics-Chemical Modeling of Wellbore Stability in Shale Formations", *Paper Presented at 45th Annual Technical Meeting of the Petroleum Society of CIM, Calgary*, June, 1994.

[3] Volk L., Carroll H., "Status Report on Modeling of Wellbore Stability", *U.S. Department of Energy, Bartlesville Project Office, Oklahoma, USA, NIPER/BDM-0199*, pp. 1-6, 1995.

[4] Lal, M., "Shale Stability: Drilling Fluid Interaction and Shale Strength", *Paper Presented at SPE Latin American and Caribbean Petroleum Engineering Conference held in Caracas, Venezuela, SPE 54356*, 1-10, April, 1999.

[5] Igbokoyi A., Rahbar N., Soboyejo W., "Rock Mechanical Properties for Borehole Stability Modeling in Niger Delta Region", *Research Proposal Submitted to Petroleum Technology Development Fund (PTDF), Nigeria*, pp. 1-18, 2012.

[6] Osisanya, S. O., "Practical Approach to Solving Wellbore Instability Problems", *Presented at SPE Distinguished Lecturer Program*, Program Year 2011-2012.

[7] Khan, S., Ansari, S. and Khosravi, N., "Prudent and Integrated Approach to Understanding Wellbore Stability in Canadian Foothills to Minimize Drilling Challenges and Non-Productive Time", *GeoConvention 2012: Vision*, pp. 3-4, 2012.

[8] Simangunsong, R. A., Villatoro, J. J., Davis, A. K., "Wellbore Stability Assessment for Highly Inclined Wells Using Limited Rock-Mechanics Data", *Paper Presented at the SPE Annual Technical Conference and Exhibition held in San Antonio, Texas, U. S. A, SPE 99644*, 1-13, September, 2006.

[9] Lowrey, J. P., Ottesen, S., "An Assessment of the Mechanical Stability of Wells Offshore Nigeria", *SPE Drilling and Completion*, pp. 34-35, March 1995.

[10] Lang J., Li S., Halliburton USA, Zhang J., Shell Exploration & Production Company, USA, "Wellbore Stability Modeling and Real-Time Surveillance for Deepwater Drilling to Weak Bedding Planes and Depleted Reservoirs", *SPE/IADC 139708*, 1-18, 2011.

[11] McLellan, P.J., "Assessing the Risk of Wellbore Instability in Horizontal and Inclined Wells", *The Journal of Canadian Petroleum Technology, Vol. 35, No. 5*, 21-32, 1996.

[12] Pasic, B., Gaurina-Medimurec, N., Matanovic, D., "Wellbore Instability: Causes and Consequences", *Rud-geol-naft.zb.*, Vol 19.2007.

[13] Mohiuddin, M. A., Awal, M. R., Abdulraheem, A., Khan, K., "A New Diagnostic Approach to Identify the Causes of Borehole Instability Problems in an Offshore Arabian Field", *Paper Presented at the SPE Middle East Oil Show, Bahrain, SPE 68095,* March 2001.

[14] Zahn, M. N., Coelho, L. C., Landau, L., and Alves, J. L. D., " Numerical Study on Wellbore Stability Analysis Considering Volumetric Failure", *Asociacion Argentina de Mecanica Computacional, Argentina,* 8837-8858, 2010. www.amcaonline.org.ar

[15] Bradley, W. B., "Failure of Inclined Boreholes", *Journal of Energy Resources Technology/Transactions of the ASME,* 232-239, 1979.

[16] Chen, S., "Analytical and Numerical Analyses of Wellbore Drilled in Elastoplastic Porous Formations", *Dissertation submitted to the graduate faculty, University of Oklahoma, USA,* 2012.

[17] McLellan, P. and Hawkes, C., "Borehole Stability Analysis for Underbalanced Drilling", *Paper Presented at the CSPG and Petroleum Society Joint Convention in Calgary, Alberta, Canada,* 1999.

[18] Morita, N., "Well Orientation Effect on Borehole Stability", *Paper Presented at the Annual Technical Conference and Exhibition held in Houston Texas, U.S.A,* SPE 89896, 2004.

[19] McLean, M.R. and Addis, M.A., "Wellbore Stability: The Effect of Strength Criteria on Mud Weight Recommendations", *Paper Presented at the 65th Annual Technical Conference and Exhibition of the Society of Petroleum Engineers held in New Orleans, LA,* 1990.

[20] Ewy, R.T., "Wellbore Stability Predictions by Use of a Modified Lade Criterion", *SPE Drill and Completion 14 (2),* 1-7, June, 1999.

[21] Hoek, E. and Brown, E. T., "Empirical Strength Criterion for Rock Masses", *Journal of Geotech Eng. Div., ASCE, 106,* pp.1013-1035, 1980.

[22] Hoek, E. and Brown, E. T., "The Hoek-Brown Failure Criterion – A 1988 Update", *Proc. 15th Canadian Rock Mechanics Symposium,* October 1988.

[23] Wang, Y. and Dusseault, M. B., "Borehole Yield and Hydraulic Fracture Initiation in Poorly Consolidated Rock Strata – Part II. Permeable Media", *International Journal of Rock Mechanics, Mining Science and Geomechanics Abstracts,* Vol. 28, No 4, 247-260, 1991.

[24] Detournay, E. and St. John, C.M., "Design Charts for a Deep Circular Tunnel under Non-Uniform Loading", *Rock Mechanics and Rock Engineering*, Vol. 21, 119-137, 1988.

[25] McLellan, P. J., and Wang, Y., "Predicting the Effects of Pore Pressure Penetration on the Extent of Wellbore Instability: Application of a Versatile Poro-Elastoplastic Model", *SPE 28053 Paper Presented at SPE/ISRM Eurock'94, Delft, the Netherlands*, August, 1994.

[26] Hawkes, C. D. and McLellan, P.J., "A New Model for Predicting Time-Dependent Failure of Shales: Theory and Application", *CIM Paper 97-131, Presented at the 48th Annual Technical Meeting of the CIM Petroleum Society, Calgary, Alberta, Canada*, June, 1997.

[27] Introduction to Numerical Modeling Exam Preparation Course (c) OHMS 2011. http://www.ohms.co.za/courses/sco/SCO-Day3-StrengthCriteria.pdf

[28] Aadnoy, B.S. and Chenevert, M. E., "Stability of Highly Inclined Boreholes", *SPE Drilling Engineering*, pp. 364-374, September, 1987.

[29] Al-Wardy, W. and Urdaneta, O. P., "Geomechanical Modeling for Wellbore Stability during Drilling Nahr Umr Shales in a field in Petroleum Development Oman', *Paper Presented at the International Petroleum Exhibition and Conference held in Abu Dhabi, UAE,* November, 2010.

[30] www.bakerhughes.com/news-and-media/resources/brochures/geomechanical-modeling

[31] Raba'a, A. S., Abass, H. H., Hembling, D. E., "A Geomechanical Facies-Based Approach to Optimize Drilling and Completion Strategy of an Unconsolidated Sandstone Reservoir, Saudi Arabia", *Paper Presented at the SPE Annual Technical Conference and Exhibition held in Anahelm, California, U. S. A.* SPE 109774, November, 2007

[32] Mohiuddin, M. A., Khan, K., Abdulraheem, A., Awal, M. R., "Analysis of Wellbore Instability in Vertical, Directional, and Horizontal wells using Field Data", *Journal of Petroleum Science and Engineering 55 (2007) 83-92.*

[33] Detournay, E. and Cheng, A.H-D., "Fundamentals of Poroelasticity", *Comprehensive Rock Engineering: Principles, Practice and Projects, Vol. II, Analysis and Design Method*, pp. 113-171, ed. C. Fairhurst, pergamon Press, 1993.

[34] Wang, Y. I., Dusseault, M. B., "A Coupled Conductive-Convective Thermo-Poroelastic Solution and Implications for Wellbore Stability", Journal of Petroleum Science and Engineering, Vol. 38: 187-198, 2003

[35] Yu, M., Chenevert, M.E., Sharma, M. M., "Chemical-Mechanical Wellbore Instability Model for Shales: Accounting for Solution Diffusion", Journal of Petroleum Science and Engineering, Vol. 38: 131-143, 2003.

[36] Zhou, X. X. and Ghassemi, A., "Chemo-Poromechanical Finite Element Modeling of a Wellbore in Swelling Shales", *Paper Presented at the 42nd US Rock Mechanics Symposium and 2nd US-Canada Rock Mechanics Symposium, held in San Francisco, U.S.A,* June-July, 2008.

[37] Fuh, G-F., Deom, D. B., Turner, R. D., "Wellbore Stability and Drilling Results From the First Horizontal Well in the Kotter Field Offshore, The Netherlands", *Paper Presented at the 66th Annual Technical Conference and Exhibition of the Society of Petroleum Engineers held in Dallas, TX., U.S.A,* SPE 22544, 1991.

[38] Santarelli, F. J., Dahen, D., BaroudI, H., Sliman, K. B., "Mechanisms of Borehole Instability in Heavily Fractured Rock Media", *International Journal of Rock Mechanics, Mining Science and Geomechanics Abstracts 29 (5),* 457-467, 1992.

[39] Ong, S. H., Roegiers, J-C., "Horizontal Wellbore Collapse in an Anisotropic Formation", *Paper Presented at the Productions Symposium held in Oklahoma City, OK., U.S.A,* SPE 25504, 1993.

[40] Morita, N., Ross, C. K., "Core-Based Horizontal or highly Inclined Well Stability Analysis for Unconsolidated Formations", *Paper Presented at the 68th Annual Technical Conference and Exhibition of the Society of Petroleum Engineers held in Houston, TX., U.S.A,* SPE 26332, 1993.

[41] Wong, S-W., Veeken, C. A. M., Kenter, C. J., "The Rock-Mechanical Aspects of Drilling and North Sea Horizontal Well", *SPE Drilling and Completion,* 1994.

[42] Marisela, S. D., Cabrera, S., Jose, R., "Geomechanical Design and Evaluation of a Horizontal Wellbore in Maracaibo Lake, Venezuela: Real-Drilling-Time Application", *Paper Presented at the SPE International Conference held in Calgary, Canada,* SPE 37088, 1996.

[43] Santarelli, F. J., Zaho, S., Burrrafato, G., Zausa, F., Giacca, D., "Wellbore Stability Analysis Made Easy and Practical", *Paper IADC/SPE 35105 Presented at IADC/SPE Conference, New Orleans, Louisiana, U.S.A,* pp. 523-532, March, 1996.

[44] Cui, L., Abousleiman, Ekbote, S., Roegiers, J-C., Zaman, M., "A Software for Poroelastic Analyses of Borehole Stability", *Paper Presented at the SPE Latin American and Caribean Petroleum Engineering Conference held in Caracas, Venezuela,* SPE 54013, 1999.

[45] Fung, L. S. K., Wan, R. G., Rodriguez, H., "An Advanced Elasto-plastic Model for Borehole Stability Analysis of Horizontal Wells in Unconsolidated Formation", *Paper Presented at the 47th Annual Technical Meeting of The Petroleum Society in Calgary, Alberta, Canada,* PAPER 96-58, 1999.

[46] Zhang, J., Roegiers, J-C., "Horizontal Borehole Stability in Naturally Fractured Reservoirs", *Paper Presented at the SPE/The Petroleum Society of CIM International Conference on Horizontal Well Technology held in Calgary, Alberta, Canada,* CIM 65513, 2000.

[47] Finkbeiner, T., Moos, D., DeRose, W., Shiflet, D., "Wellbore Stability Evaluation for Horizontal Completion – A Case Study", *Paper Presented at the SPE Asia Pacific Oil and Gas Conference and Exhibition held in Brisbane, Australia,* SPE 64409, 2000.

[48] Saidin, S., Smith, S. P.T., "Wellbore Stability and Formation Damage Considerations for Bakok Field K Formation", *Paper IADC/SPE 62797 Presented at IADC/SPE Asia Pacific Drilling Technology Conference, Kuala Lumpur,Malaysia,* pp. 1-11, September, 2000.

[49] Onaisi, A., Locane, J., Razimbaud, A., "Stress Related Wellbore Instability Problems in Deep Wells in ABK Field", *Paper Presented at the 9th Abu Dhabi International Petroleum Exhibition and Conference, Abu Dhabi, UAE,* pp. 1-8, October, 2000.

[50] Mody, F. K., Tare, U., Wang, G., "Sustainable Deployment of Geomechanics Technology to Reducing Well Construction Costs", *Paper Presented at the SPE/IADC Middle East Drilling Technology Conference and Exhibition held in Cairo, Egypt*, SPE/IADC 108241, 2007.

[51] Sinha, K. B., Wang, J., Kisra, S., Li, J., Pistre, V. Bratton, T., Sanders, M., " Estimation of Formation Stresses Using Borehole Sonic Data", *Paper Presented at the SPWLA 49th Annual Logging Symposium held in Edinburgh, Scotland,* 2008.

[52] Nguyen, V. X., Abousleiman, Y., "The Porochemothermoelastic Coupled Solutions of Stress and Pressure with Applications to Wellbore Stability in Chemically Active Shale", *Paper Presented at the SPE Annual Technical Conference and Exhibition held in New Orleans, Louisiana, U.S.A,* SPE 124422, 2009.

[53] Furul, K., Fuh, G-F., Abdelmalek, N., "Acomprehensive Modeling Analysis of Borehole Stability and Production Liner Deformation for Inclined/Horizontal Wells Completed in a Highly Compacting Chalk Formation", *Paper Presented at the SPE Annual Technical Conference and Exhibition held in New Orlean, Lousiana, U.S.A,* SPE 123651, 2009.

[54] Soreide, O. K., Bostrom, B., Horsrud, P., "Borehole Stability Simulation of an HPHT Field using Anisotropic Shale Modeling", *Paper Presented at Asheville 43rd US Rock Mechanics Symposium and 4th US-Canada Rock Mechanics Symposium held in Asheville, ARMA 09-185,* 2009.

[55] Li, S., Purdy, C., "Maximum Horizontal Stress and Wellbore Stability White Drilling: Modeling and Case Study", *Paper Presented at the SPE Latin American and Caribean Petroleum Engineering Conference held in Lima Peru,* SPE 139280, 2010.

[56] www.tech.plym.ac.uk/sme/interactive_resources/tutorials (Fracture Mechanics Tutorials by Prof M Neil James).

[57] en.wikipedia.org/wiki/Fracture_mechanics

[58] Wang, C. H., "Introduction to Fracture Mechanics", *Published by DSTO Aeronautical and Maritime Research Laboratory, Melbourne Victoria, Australia,* July, 1996.

[59] ksm.fsv.cvut.cz/~sejnom/download/pm10_tisk.pdf (Fracture Mechanics).

[60] http://www.efunda.com/formulae/solid_mechanics/fracture_mechanics/fm_intro.cfm.

[61] Callister, W. D., "Materials Science and Engineering: An Introduction", *Published by John Wiley & Sons, Inc., New york, USA, 7th Edition*, pp. 209 -218, 2007.

[62] Dieter, G. E., "Mechanical Metallurgy", *Published by McGraw-Hill Book Co, UK, SI Metric ed.,* pp.241, 246-247, 362-366, 1988.

[63] Rinne, M., "Fracture Mechanics and Subcritical Crack Growth Approach To Model Time-Dependent Failure in Brittle Rock", *Doctoral Dissertation Submitted To the Faculty of Engineering and Architecture, Helsinki University of Technology, Espoo, Finland*, August, 2008.

[64] Kabiru, M., "Strength and Fracture of Earth-Based and Natural Fiber-Reinforced Composites", *Unpublished MSc Thesis Submitted To the Graduate Faculty of Material Science and Engineering Stream, African University of Science and Technology, Abuja*, pp. 17-18, 2010.

[65] Backers, T., "Fracture Toughness Determination and Micromechanics of Rock Under Mode I and Mode II Loading", *Doctoral Dissertation Submitted to the University of Potsdam, Germany,* pp. 5-8, August, 2004.

[66] Soboyejo, W., "Mechanical Properties of Engineered Materials", *Published by Marcel Dekker, Inc., New York, USA,* pp. 317-332, 338-344, 2003.

[67] Griffith, A. A., "The Phenomena of Rupture and Flow in Solids", *Phil. Trans. Royal Soc. London; Series A,* 221, pp. 163-198 1920.

[68] Inglis, C.E., Trans Inst Naval Architects, Vol. 55, pp. 219–224, 1913.

[69] Orowan, E., "Fatigue and Fracture of Metals". *MIT Press, Cambridge, MA, USA,* p.139, 1950.

[70] Irwin G R., "Analysis of Stresses and Strains near the End of a Crack Transversing a Plate", *J. Appl. Mech., 24,* p. 361-370, 1957.

[71] Wells A.A., Proc. of Crack Propagation Symposium, Cranfield College of Astronau-tics,1, p. 210, 1961.

[72] Cottrell, A.H. (1961) Iron and Steel Institute. Special Report, Vol. 69, p. 281.

[73] Rice, J.R., J Applied Mech. vol. 35, pp. 379–386, 1968.

CHAPTER THREE

3.0 Numerical Modeling of Wellbore Instability (Shear Failure) Using Fracture Mechanics Approach

A typical wellbore consists of various layers of rock formations having pre-existing cracks and distinct mechanical properties. Considering a wellbore having different layers with each layer made up of rock formations (typically shales, as found in Niger-Delta region of Nigeria). The shales will certainly have pre-existing cracks, of which some will be inclined at an angle. Upon the application of compressive load on the formation, the inclined cracks are susceptible to making the formation fail in shear.

In order to gain useful insights to guide us in the assessment or prediction shear failure wellbore instability, a fracture mechanics approach using the linear elastic fracture mechanics (LEFM) concept was employed in this study. This was done by assuming that the rock formation is linear and elastic and contains inherent pre-existing cracks. This simplicity provides a conservative approach to the prediction of wellbore instability. It can also be used to determine the lower bound mud weight window for safe drilling operations in conventional wells.

This chapter presents the procedures used for the numerical modeling of a typical wellbore wall containing pre-existing cracks. The diagrammatic views of the modeled wellbore are displayed.

3.1 Numerical Modeling Procedures of a Typical Wellbore Wall Using ABAQUS

The commercially available ABAQUS^{TM} 6.12 finite element software package (teaching edition) was used in this work. LEFM concept was employed in this study by assuming that the rock formation is linear, elastic and contains inherent pre-existing cracks. This simplicity provides a conservative approach for the prediction of well bore instability. It will also be used to determine the lower bound mud weight window for safe drilling operations.

3.1.1 Model Geometry

Two-dimensional planar deformable shell geometry was used for the modeling. One part of the wellbore wall was modeled, due to symmetry. The dimension of the modeled part was 40 inches by 15 inches. Figure 4.1 shows the two dimensional model geometry of the wellbore part used in this study.

3.1.2 Material properties

The material was assumed to be isotropic. It was also assumed to be linear, elastic with Young's modulus, E = 432,825 psi and Poisson's ratio, v = 0.25 ((based on the oil field data used for this work- see appendix).

3.1.3 Inclined Crack Insertion

Cracks of different lengths (0.5 – 2.5) inches inclined at 30^0 to the horizontal plane were inserted on the wellbore wall.

3.1.4 Element Selection and Meshing

The wellbore wall was meshed using the Quad structured 4-noded solid elements and analyzed using the plane strain assumptions.

3.1.5 Boundary Conditions and Pressure Application

The wellbore part was constrained by applying symmetry boundary conditions along the wall thickness on both edges. It was then loaded with pressure ranging from 3000-7000 psi.

Figure 3.1: A Schematic View of the Two Dimensional Model Geometry of the Wellbore Part

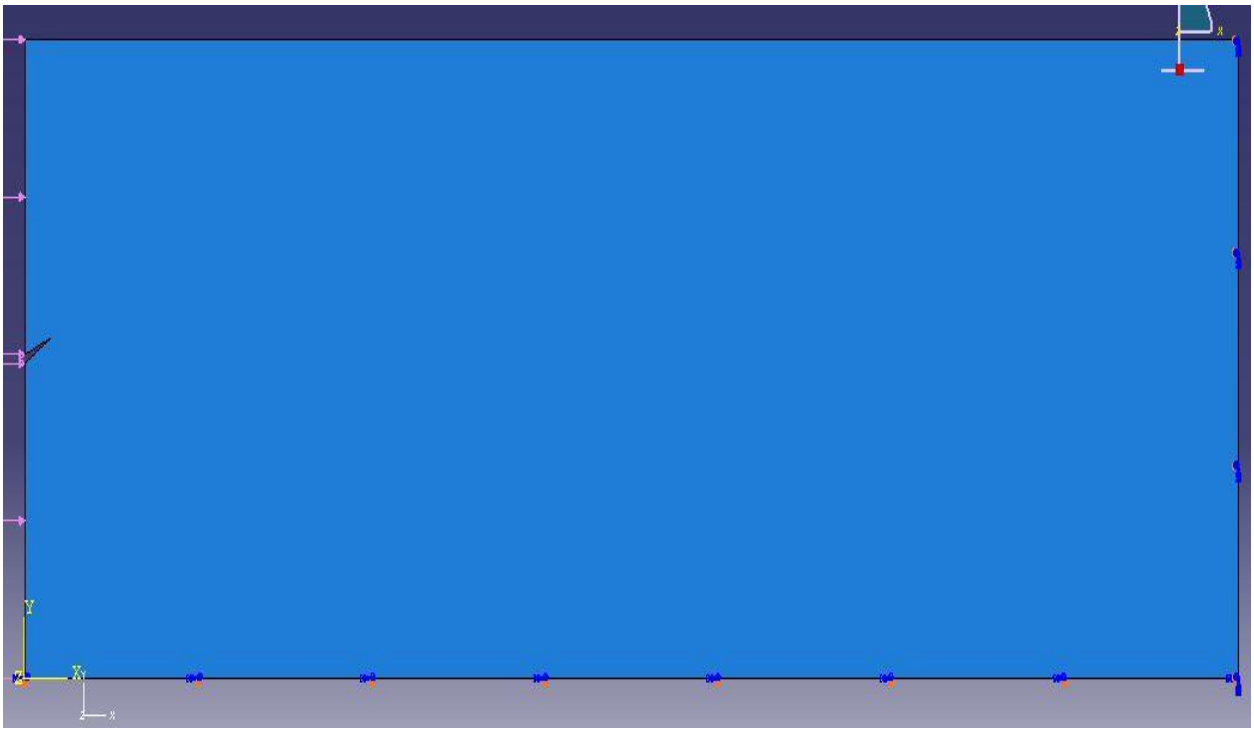

Figure 3.2: A Schematic View Showing the Boundary Conditions and Applied Pressure Loading of the Modeled Wellbore Wall

CHAPTER FOUR

4.0 Results and Discussion

With the aid of commercially available ABAQUS^{TM} 6.12 finite element software, essential fracture mechanics parameters were obtained from the modeled wellbore wall. Based on the drilling scenario considered in this work, these parameters were used to predict the drilling pressure for the onset of shear failure of wellbores. The obtained pressure was also used to determine the lower bound mud weight window that can be used for safe drilling operations.

4.1 Results Obtained From ABAQUS

The results obtained from ABAQUS are presented in Table 4.1. These show the values of the J integral obtained from the modeled well bore. J integral was used because of its convergence.

Table 4.1: Result obtained from ABAQUS

Pressure (psi)	**J at 0.5in Crack length (lbf/in)**	**J at 1in Crack length (lbf/in)**	**J at 1.5in Crack length (lbf/in)**	**J at 2in Crack length (lbf/in)**	**J at 2.5in Crack length (lbf/in)**
3000	1.53062	5.001	8.68899	12.5528	16.6876
3500	2.08335	6.80169	11.8267	17.0857	22.7137
4000	2.7211	8.88384	15.4471	22.316	29.6668
4500	3.4439	11.2436	19.5502	28. 2437	37.5471
5000	4.25172	13.881	24.1361	34.8688	46.3544
5500	5.14459	16.796	29.2046	42.1913	56.0888
6000	6.12248	19.9886	34.7559	50.2111	66.7504
6500	7.18541	23.4589	40.79	58.9283	78.339
7000	8.33338	27.2068	47.3067	68.3429	90.8546

For *linear elastic* materials, $-\frac{1}{B}\frac{d\Pi}{da} = G$, which means that J = G for the linear elastic case, where J represents the J integral and G, the strain energy release rate. Also under small scale yielding (LEFM), J is uniquely related to stress intensity factor, K following Irwin [1] proposition on the relationship between the strain energy release rate, G, and the stress intensity factor, K, for the three modes of fracture as follows:

$$J_I = G_I = \frac{K_I^2}{E'} \tag{4.1}$$

$$J_{II} = G_{II} = \frac{K_{II}^2}{E'} \tag{4.2}$$

$$J_{III} = G_{III} = \frac{K_{III}^2}{2\mu} \tag{4.3}$$

where J_I, J_{II}, J_{III} and G_I, G_{II}, G_{III} are the J integral and the strain energy release rates for Mode I, Mode II, and Mode II, respectively, $\mu = E/2(1+v)$, $E' = \frac{E}{(1-v^2)}$ for plane strain, and $E' = E$ for plane stress, where E is the Young's modulus, v is Poisson's ratio.

When a crack extends along its own plane and is exposed to a Mixed-mode I-II loading (as the case we are considering), the overall strain energy release rate, G, is a summation of the Mode I strain energy release rate, G_I, and that of Mode II, G_{II} [2]. Hence, we obtain:

$$J = G = \frac{K_{eff}^2}{E'} \tag{4.4}$$

where $J = J_I + J_{II}$, $G = G_I + G_{II}$, and $K_{eff}^2 = K_I^2 + K_{II}^2$, K_{eff} can be referred to as the effective stress intensity factor.

By implication, $K_{eff} = \sqrt{K_I^2 + K_{II}^2}$, (4.5)

Since the wellbore wall has a very large diameter, we considered a plane strain condition in this study. Hence, equation 4.4 may be expressed as:

$$J = G = \frac{K_{eff}^2}{E}(1 - v^2) \tag{4.6}$$

4.2 Determination of the Effective Stress Intensity Factor, K_{eff}.

Using the concept of LEFM (as summarized in equation 4.6) and from the results obtained from ABAQUS (Table 4.1), we can obtain the effective stress intensity factors, $K_{eff,}$ for the wellbore formation as pressure is applied to it. Table 4.2 shows the different pressure ranges used in this study with the obtained corresponding effective stress intensity factors, $K_{eff,}$ for the two possible modes of fracture that can occur within the wellbore wall considering various inherent pre-existing crack lengths. The values of the Young modulus (E) and Poisson ratio (v) of the well bore formation used for the computation of the K_{eff} are 432,825 psi and 0.25 respectively.

Table 4.2: Effective Stress Intensity Factors, K_{eff} of the Wellbore Formation at Different Crack Lengths and Pressure

Pressure (psi)	**K_{eff} at 0.5in Crack length ($psi\text{-}in^{1/2}$)**	**K_{eff} at 1in Crack length ($psi\text{-}in^{1/2}$)**	**K_{eff} at 1.5in Crack length ($psi\text{-}in^{1/2}$)**	**K_{eff} at 2in Crack length ($psi\text{-}in^{1/2}$)**	**K_{eff} at 2.5in Crack length ($psi\text{-}in^{1/2}$)**
3000	840.6	1519.5	2002.9	2407.4	2775.7
3500	980.7	1772.1	2336.7	2808.6	3238.3
4000	1120.8	2025.2	2670.5	3209.8	3700.9
4500	1260.9	2278.4	3004.3	3611	4163.5
5000	1401	2531.5	3338.1	4012.3	4626.1
5500	1541.2	2784.7	3671.9	4413.5	5088.7
6000	1681.3	3037.8	4005.8	4814.7	5551.3
6500	1821.4	3291	4339.6	5215.9	6013.9
7000	1961.5	3544.1	4673.4	5617.2	6476.6

Figure 4.1 shows a graph plot of the effective stress intensity factor, K_{eff}, against the different crack lengths. The plot will guide us in predicting the onset of shear failure wellbore instability.

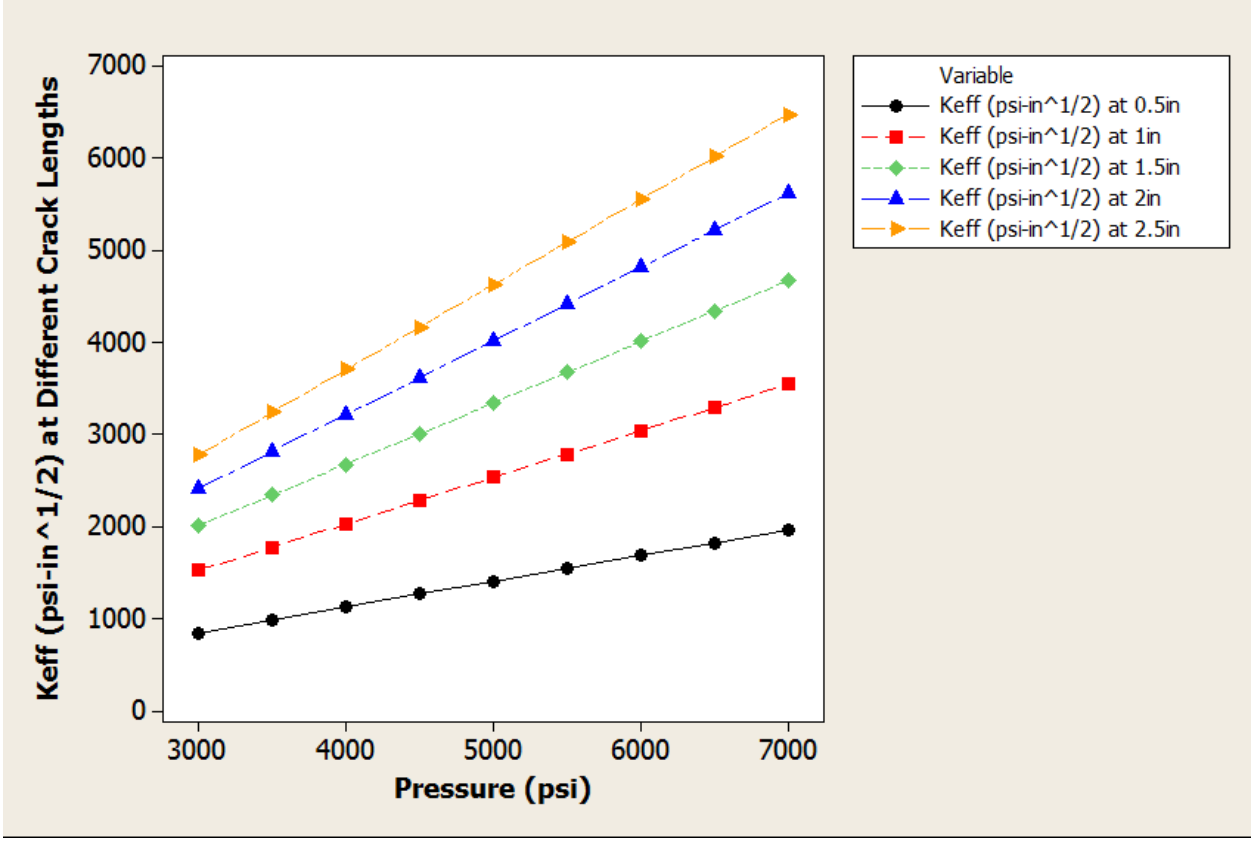

Figure 4.1: Graph of Effective Stress Intensity Factor at Different Crack Lengths against Pressure

4.3 Prediction of the Drilling Pressure for the Onset of Shear Failure Wellbore Instability

The drilling pressure for the onset of shear failure wellbore instability at different crack lengths can be predicted from the graph of the effective stress intensity factor, K_{eff}, against the pressure ranges applied. By fixing in the value of the critical effective stress intensity factor, K_{effc}, for a mixed mode I-II, which is obtained from $\sqrt{K_{IC}^2 + K_{IIC}^2}$ into the graphical equation, we can obtain the corresponding pressure for the onset of shear failure.

According to Fischer, M. P., et al. 2008 [3], the value of typical value of the fracture toughness (K_{IC}) of shales obtained from various sources is about 0.9 MPa-$m^{1/2}$ (818.89 psi-$in^{1/2}$). In general K_{IIC} is larger than K_{IC} in rock, a factor of 2-3 is usually assumed for ambient condition [4, 5]. If we are to consider an average value, then, K_{IIC} = 2.5 K_{IC} = 2,047.22 psi-$in^{1/2}$. Therefore, the critical effective stress intensity factor, $K_{effc} \approx \sqrt{K_{IC}^2 + K_{IIC}^2}$ = 2,204.92 psi-$in^{1/2}$.

4.3.1 Prediction of the Drilling Pressure for the Onset of Shear Failure Wellbore Instability at a Crack Length of 0.5 inch

Figure 4.2 shows a plot of the effective stress intensity factor, K_{eff}, against the pressure ranges applied at a crack length of 0.5 inch.

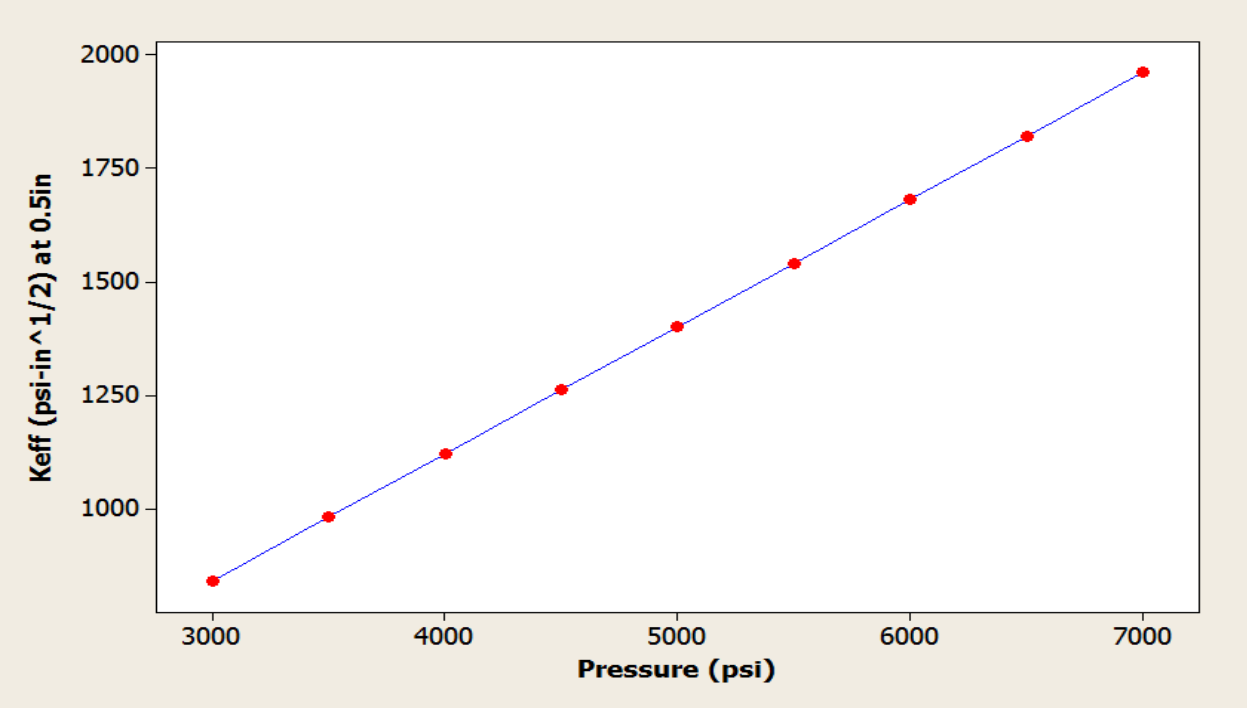

Figure 4.2: Graph of Effective Stress Intensity Factor at 0.5 inch Crack Length against Pressure

The equation for the graph is: K_{eff} = - 0.122 + 0.280 P (4.7)

where P is the pressure and K_{eff} is the effective stress intensity factor.

At the critical effective stress intensity factor, K_{effc}, value, which is 2,204.92 psi-$in^{1/2}$, the drilling pressure for the onset of instability will, therefore, be **7,875.16 psi**.

4.3.2 Prediction of the Drilling Pressure for the Onset of Shear Failure Wellbore Instability at a Crack Length of 1 inch

Figure 4.3 shows a plot of the effective stress intensity factor, K_{eff}, against the pressure ranges applied at a crack length of 1 inch.

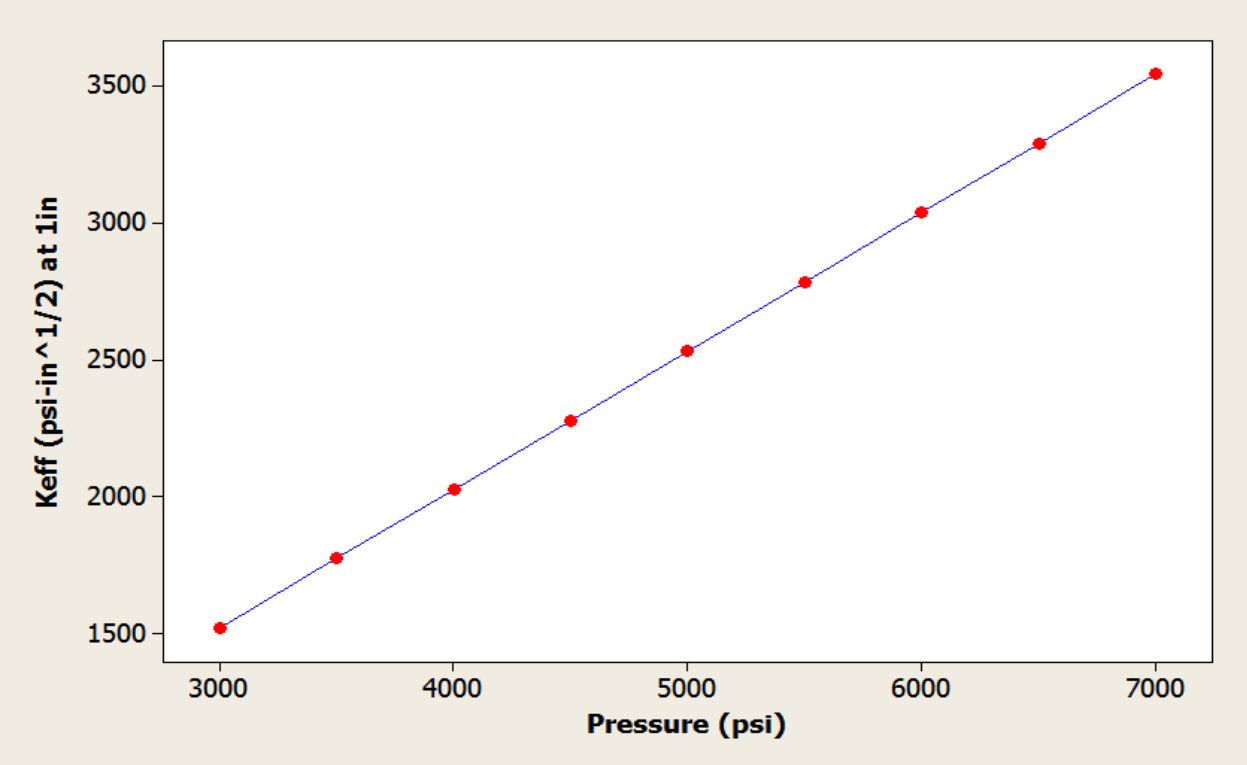

Figure 4.3: Graph of Effective Stress Intensity Factor at 1 inch Crack Length against Pressure

The equation for the graph is: $K_{eff} = 0.489 + 0.506\ P$ (4.8)

where P is the pressure and K_{eff} is the effective stress intensity factor.

At the critical effective stress intensity factor, K_{effc}, value, which is 2,204.92 psi-in$^{1/2}$, the drilling pressure for the onset of instability will, therefore, be **4,356.58 psi**.

4.3.3 Prediction of the Drilling Pressure for the Onset of Shear Failure Well Bore Instability at a Crack Length of 1.5 inches

Figure 4.4 shows a plot of the effective stress intensity factor, K_{eff}, against the pressure ranges applied at a crack length of 1.5 inches.

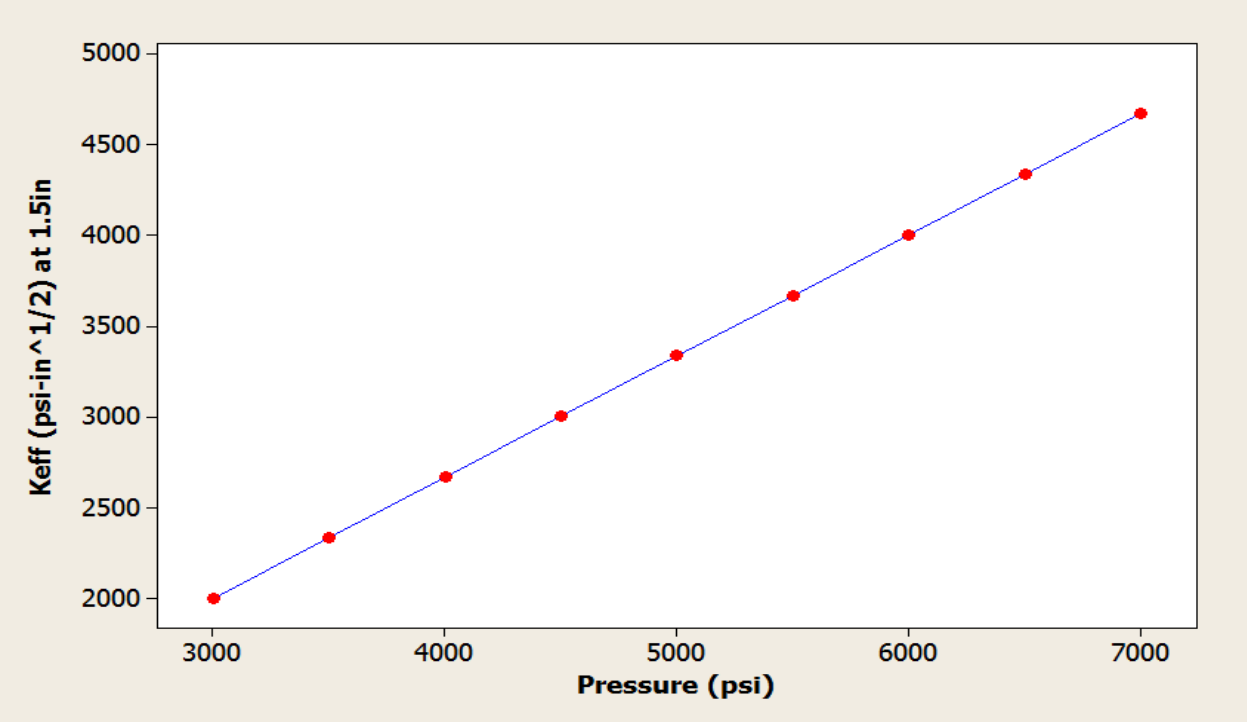

Figure 4.4: Graph of Effective Stress Intensity Factor at 1.5 inches Crack Length against Pressure

The equation for the graph is: $K_{eff} = -0.0167 + 0.668\ P$ (4.9)

where P is the pressure and K_{eff} is the effective stress intensity factor.

At the critical effective stress intensity factor, K_{effc}, value, which is 2,204.92 psi-in$^{1/2}$, the drilling pressure for the onset of instability will, therefore, be **3,300.8 psi**.

4.3.4 Prediction of the Drilling Pressure for the Onset of Shear Failure Well Bore Instability at a Crack Length of 2 inches

Figure 4.5 shows the graph of the effective stress intensity factor, K_{eff}, against the pressure ranges applied at a crack length of 2 inches.

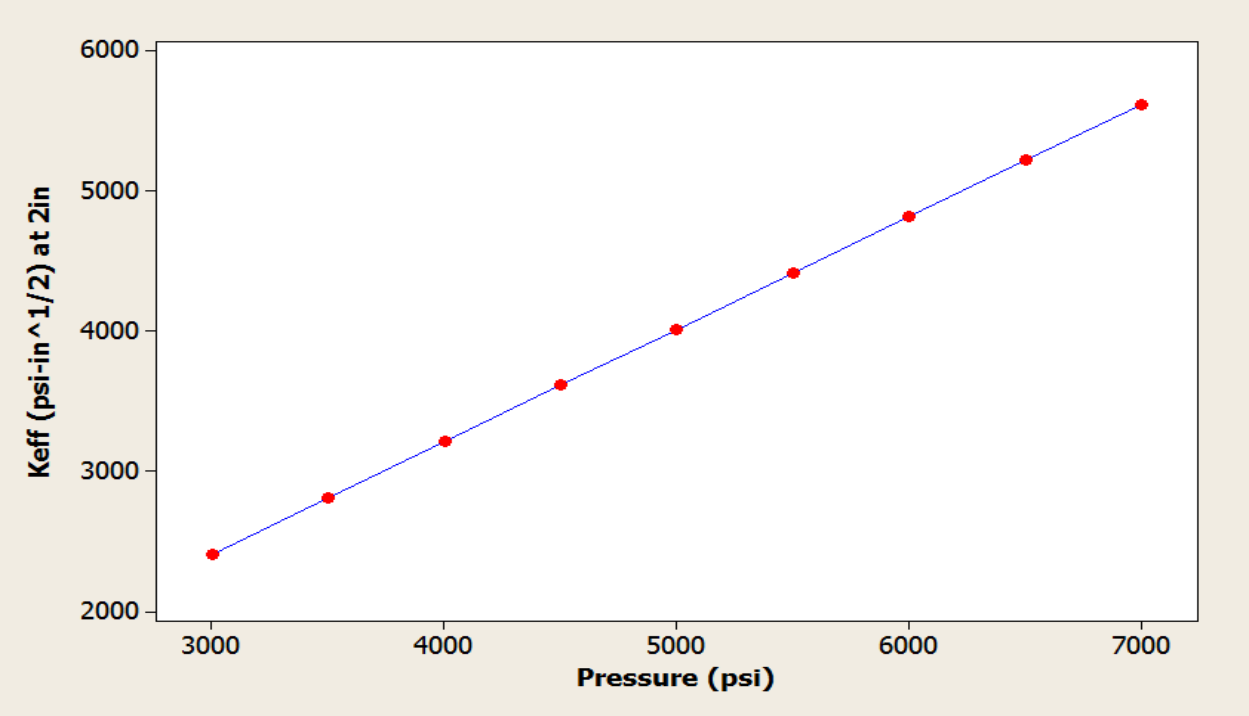

Figure 4.5: Graph of Effective Stress Intensity Factor at 2 inches Crack Length against Pressure

The equation for the graph is: $K_{eff} = 0.0333 + 0.802\ P$ (4.10)

where P is the pressure and K_{eff} is the effective stress intensity factor.

At the critical effective stress intensity factor, K_{effc}, value, which is 2,204.92 psi-in$^{1/2}$, the drilling pressure for the onset of instability will, therefore, be **2,749.24 psi**.

4.3.5 Prediction of the Drilling Pressure for the Onset of Shear Failure Well Bore Instability at a Crack Length of 2.5 inches

Figure 4.6 shows the graph of the effective stress intensity factor, K_{eff}, against the pressure ranges applied at a crack length of 2.5 inches.

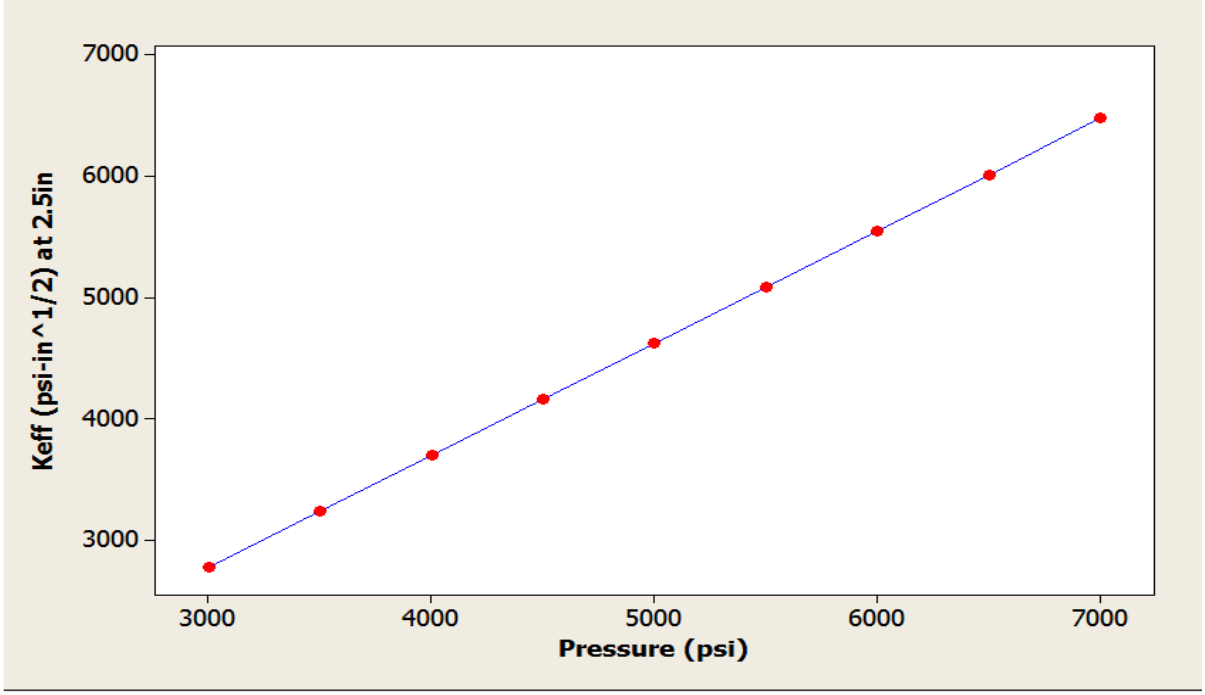

Figure 4.6: Graph of Effective Stress Intensity Factor at 2.5 inches Crack Length against Pressure

The equation for the graph is: $K_{eff} = 0.0444 + 0.925\ P$ (4.11)

where P is the pressure and K_{eff} is the effective stress intensity factor.

At the critical effective stress intensity factor, K_{effc}, value, which is 2,204.92 psi-in$^{1/2}$, the drilling pressure for the onset of instability will, therefore, be **2,383.65 psi**.

4.3.6 Effect of Increase in Crack Length on the Drilling Pressure

From the obtained results of the drilling pressure for the onset of shear failure at different crack lengths, it was observed that as the crack length increases, the drilling pressure reduces. This clearly shows the effect of crack size in the wellbore formation during drilling. Table 4.3 and Figure 4.7 shows the relationship between the drilling pressure and the different crack lengths.

Table 4.3: Drilling Pressure for the Onset of Shear Failure at Different Crack Lengths

Drilling Pressure (psi)	Crack Length (in)
7,875.16	0.5
4,356.58	1
3,300.8	1.5
2,749.24	2
2,383.65	2.5

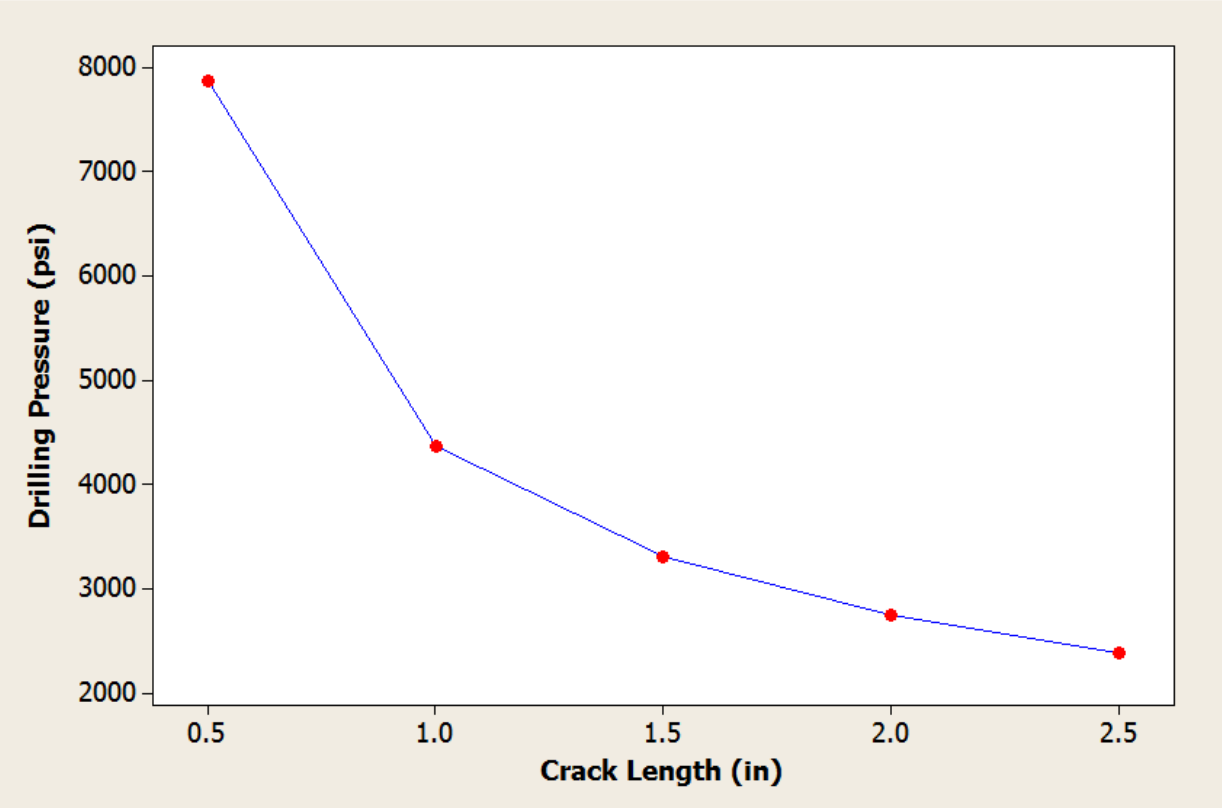

Figure 4.7: Graph of Effective Drilling Pressure Against Different Crack Lengths

4.4 Determination of the Lower Bound Mud Weight Window

The lower bound for a safe mud weight window that can be used during drilling operations can be determined from the obtained values of the drilling pressure at the onset of shear failure. Equation 4.12 [6] shows the relationship between the drilling pressure and mud weight.

$$\text{Mud weight (ppg)} = \frac{\text{Pressure (psi)}}{0.052 \div \text{TVD (ft)}} \tag{4.12}$$

where TVD is the true vertical depth of the well.

From the above relationship, the lower bound mud weight at the different crack lengths using a TVD value of 12584 feet obtained from the oil field data used for this work is shown below:

Table 4.4: Lower Bound Mud Weight at Different Crack Lengths

Crack Length (in)	Drilling Pressure (psi)	Lower Bound Mud Weight (ppg)
0.5	7,875.16	12.03
1	4,356.58	6.66
1.5	3,300.8	5.04
2	2,749.24	4.20
2.5	2,383.65	3.64

4.5 Implications of Results Obtained

This study gives us a guide on how to obtain the J integral values and the stress intensity factors associated with a wellbore that always contain inherent pre-existing cracks. By using the obtained fracture mechanics parameters, it is possible to determine the drilling pressure for the onset of shear failure around a wellbore, as have been shown in this work. Furthermore, the lower bound mud weight that can be used for safe drilling operations may be obtained from the calculated drilling pressure. By using linear elastic fracture mechanics concept, this work clearly shows how we can develop a numerical model that provides a conservative approach for the prediction of wellbore instability.

4.6 References

[1] Irwin G R., "Analysis of Stresses and Strains near the End of a Crack Transversing a Plate", *J. Appl. Mech., 24,* p. 361-370, 1957.

[2] Rinne, M., "Fracture Mechanics and Subcritical Crack Growth Approach To Model Time-Dependent Failure in Brittle Rock", *Doctoral Dissertation Submitted To the Faculty of Engineering and Architecture, Helsinki University of Technology, Espoo, Finland*, August, 2008.

[3] Fischer, M. P., Gross M. R., Engelder T.,Greenfield R. J., "Finite-Element Analysis of the Stress Distribution Around a Pressurized Crack in a Layered Elastic Medium:Implications for the Spacing of Fluid-Driven Joints in Bedded Sedimentary Rock", *Tectonophysics 247 (1995) 49-64*.

[4] Rao, Q., Sun, Z., Stephansson, O., Li, C., Stillborg, B., "Shear Fracture (Mode II) of Brittle Rock", *Int. J. Rock Mech. Min. Sci.; 40: 355-375,* 2003.

[5] Backers, T., "Fracture Toughness Determination and Micromechanics of Rock Under Mode I and Mode II Loading", *Doctoral Dissertation Submitted to the University of Potsdam, Germany*, pp. 5-8, August, 2004.

[6] Lapeyrouse, N. J., "Formulas and Calculations for Drilling, Production, and Work over", Gulf Professional Publishing, Elsevier Science, 2nd Edition, USA, p. 4, 2002.

CHAPTER FIVE

5.0 Concluding Remarks and Suggested Future Work

5.1 Concluding Remarks

In this work, wellbore instability, precisely shear failure, using linear elastic fracture mechanics approach was modeled numerically. The effective stress intensity factors for the two possible modes of fracture (Mode I and II) within a typical pressurized wellbore formation having pre-existing inclined cracks were determined. It was observed that the effective stress intensity factors increase linearly with applied pressure on the wellbore.

The drilling pressure for the onset of shear failure within the wellbore was determined for different pre-existing inclined crack lengths using the concept of the effective stress intensity factor and its critical value. It was observed that increase in an inclined crack length within a wellbore formation decreases the drilling pressure needed for the onset of shear failure.

The lower bound mud weight window that can be used for safe drilling operations in conventional wells based on the model considered were determined.

5.2 Suggested Future Work

i. There is a need to validate the results obtained from the numerical model using the linear elastic constitutive model and the borehole failure criteria (Modified Lade Criterion or Mohr-Coulomb).

ii. After a rock has been stressed beyond its peak strength level, it does not necessarily fail completely and detach from the borehole wall. In order to assess the mechanical integrity of a wellbore more realistically by incorporating its plastic behavior, the numerical modeling of the wellbore failure using elastic-plastic fracture mechanics approach should be studied. The results obtained can as well be validated using elastic-plastic constitutive models.

iii. Nano-indentation techniques can be employed to obtain the mechanical properties of the rock formation from cuttings. This will reduce the cost associated with conventional method of measuring the mechanical properties of the rock formation, which is usually by extracting core samples.

APPENDIX: Oil Field Data

Shale/ Sand Name	**Bottom Shale/ Sand Depth**	**SHALE/ SAND THICKNESS**	**Top Shale/ Sand Depth**	**PRESSURE GRADIENT**	**UCS**	**YOUNG'S MODULUS**	**POISSON RATIO**	**COHESION**	**FRICTION ANGLE**	VERT	MAX	MIN
	fttvd			psi/ft		Mpa		Mpa	degrees	psi/ft	psi/ft	psi/ft
C4200	8240	250	8490	0.45	19.36	1936	0.25	6.1	25.38	0.908	0.838	0.788
C5000	8710	20	8730	0.45	29.85	2985	0.25	9.2	26.67	0.913	0.843	0.793
shale	9283	300	9583	0.45	15.35	1535	0.25	4.9	24.89	0.919	0.850	0.800
D1000 Shale	9753	200	9953	0.45	19.15	1915	0.25	6.1	25.36	0.923	0.856	0.806
D2000 Shale	10043	60	10103	0.45	19.15	1915	0.25	6.1	25.36	0.926	0.861	0.811
D6000 Shale	10347	380	10727	0.45	19.36	1936	0.25	6.1	25.38	0.929	0.865	0.815
D7000 Shale	10917	461	11378	0.45	26.13	2613	0.25	8.1	26.21	0.934	0.874	0.824
E1000 Shale	12584	80	12664	0.49	29.85	2985	0.25	9.2	26.67	0.947	0.903	0.853
E2000 Shale	13204	247	13451	0.49	41.07	4107	0.25	12.3	28.05	0.951	0.914	0.864
E3000 Shale	13614	100	13714	0.49	34.21	3421	0.25	10.4	27.21	0.954	0.922	0.872
E6000 Shale	14368	100	14468	0.49	54.28	5428	0.25	15.8	29.68	0.959	0.937	0.887
E7000 Shale	14498	72	14570	0.49	54.33	5433	0.25	15.8	29.68	0.960	0.939	0.889
E8000 Shale	14800	270	15070	0.49	41.08	4108	0.25	12.3	28.05	0.962	0.945	0.895
F1 Shale	15391	135	15526	0.765	41.69	4169	0.25	12.5	28.13	0.966	0.957	0.907
XF200 Shale	16152	16	16168	0.86	34.30	3430	0.25	10.5	27.22	0.970	0.973	0.923
XF3000 Shale	16296	578	16874	0.905	28.28	2828	0.25	8.8	26.48	0.971	0.976	0.926
XF4000 Shale	17002	75	17077	0.887	30.45	3045	0.25	9.4	26.75	0.975	0.990	0.940
TD	17077		17077	0.877	31.64	3164	0.25	9.7	26.89	0.976	0.992	0.942

* E1000 Shale parameters were used for this work.